

Selective Hydrosilylation of Olefins by a Two-Dimensional Rh(I) Low-Valent Metal–Organic Framework

Dipendu Mandal, Madison R. Esposito, Samuel E. Griffin, Grant P. Domecus, and Seth M. Cohen^{*a}

^a Department of Chemistry and Biochemistry, University of California, San Diego, 9500 Gilman Drive, La Jolla, California 92093-0358

SUPPORTING INFORMATION

Table of Contents

Experimental	5
General information for synthesis	5
General information for material characterization	5
Synthesis of C1	5
Synthesis of C1-Rh single crystals	6
Scaled up synthesis of C1-Rh	6
Synthesis of C1-Rh with modulator	7
Synthesis of C1-Ir single crystals	7
Synthesis of C1-Ir with modulator	7
Optimization conditions for hydrosilylation of 1-Octene with Et ₃ SiH	8
Procedure for examining the scope of hydrosilylation with C1-Rh	8
Filter Test of C1-Rh LVMOF for hydrosilylation of 1-Octene with Et ₃ SiH	9
Recyclability of C1-Rh for hydrosilylation of 1-Octene with Et ₃ SiH	9
Supplementary Figures	10
Figure S1. IR spectra of C1-Rh (blue), Sn1-Rh (black) and [Rh(CO)Cl(PPh ₃) ₂] (red)	10
Figure S2. IR spectra of C1-Ir synthesized with the use of 4-equiv. tri(<i>o</i> -tolyl)phosphine	10
Figure S3. Simulated PXRD patterns of C1-Rh (red), Sn1-Rh (blue), C1-Ir (magenta) and Sn1-Ir (orange) and experimental PXRD pattern of C1-Rh (black) and C1-Ir (green)	11
Figure S4. Simulated PXRD patterns of C1-Rh (red) and experimental PXRD pattern of C1-Rh SCXRD synthesis (black), C1-Rh scale-up synthesis (blue), C1-Rh 4.0 equiv. tri(<i>o</i> -tolyl)phosphine synthesis	11
Figure S5. Air stability of C1-Rh as determined by PXRD after three months of exposure to ambient air	12
Figure S6. Air stability of C1-Rh as determined by IR analysis after three months of exposure to ambient air	12
Figure S7. Simulated PXRD patterns of C1-Ir (pink) and experimental PXRD pattern of C1-Rh 4.0 equiv. tri(<i>o</i> -tolyl)phosphine synthesis (black)	13
Figure S8. Thermogravimetric analysis of C1-Rh (blue) and [Rh(CO)Cl(PPh ₃) ₂] (black)	13
Figure S9. Thermogravimetric analysis of C1-Ir	14
Figure S10. Air stability of C1-Ir as determined by PXRD after one month of exposure to ambient air	14
Figure S11. Air stability of C1-Ir as determined by IR analysis after one month of exposure to ambient air	15
Figure S12. N ₂ adsorption and desorption isotherm of C1-Rh at 77K	15
Figure S13. Wireframe images of C1-Rh extended structure viewed along (A) the crystallographic a-axis, (B) the b-axis, and (C) the c-axis	16
Figure S14. Space-filling images of C1-Rh extended structure viewed along (A) the crystallographic a-axis, (B) the b-axis, and (C) the c-axis	16
Figure S15. Images of dry and powdery sample of C1-Rh in a 20 mL vial with side view (<i>left</i>) and top view (<i>right</i>)	17
Figure S16. SEM images of C1-Rh synthesized without modulator in THF, 80 °C for 7 d	17
Figure S17. Wireframe images of C1-Ir extended structure viewed along (A) the crystallographic a-axis, (B) the b-axis, and (C) the c-axis	18

Figure S18. Spacefill images of C1-Ir extended structure viewed along (A) the crystallographic <i>a</i> -axis, (B) the <i>b</i> -axis, and (C) the <i>c</i> -axis.	18
Figure S19. SEM images of C1-Ir synthesized without modulator in THF, 80 °C for 5 d.	19
Figure S20. SEM images of Sn1-Rh synthesis adopted from <i>Angew. Chem. Int. Ed.</i> 2022, 61, e202115454.....	19
Figure S21. ¹ H NMR spectrum of the crude mixture for the control reaction (1-octene, Et ₃ SiH) in d ₈ -toluene at 80 °C, 24 h (anisole as a reference standard).....	20
Figure S22. ¹ H NMR spectrum of the crude mixture of 1-octene, Et ₃ SiH, C1-Rh (cat) in toluene at 80 °C, 24 h (anisole as reference standard).	20
Figure S23. PXRD patterns of C1-Rh before hydrosilylation (blue) and after three rounds (3x) of hydrosilylation (red) of 1-octene with Et ₃ SiH at 80 °C for 24 h in toluene.	21
Figure S24. GCMS trace for the control of 1-octene and Et ₃ SiH in toluene at 80 °C, 24 h (<i>n</i> -dodecane internal standard).....	22
Figure S25. GCMS trace for 1-octene, Et ₃ SiH, Rh-C1 (cat) in toluene at 25 °C, 24 h.....	22
Figure S26. GCMS trace for 1-octene, Et ₃ SiH, C1-Rh (cat) in toluene at 80 °C, 24 h (red asterisk = Hydrolysis product of Et ₃ SiH; HS = Hydrosilylation; DS = Dehydrogenative Silylation).	23
Figure S27. GCMS trace for 1-octene, Et ₃ SiH, C1-Rh (cat) in benzene at 80 °C, 24h (red asterisk = Hydrolysis product of Et ₃ SiH; HS = Hydrosilylation; DS = Dehydrogenative Silylation).	23
Figure S28. GCMS trace for 1-octene, Et ₃ SiH, C1-Rh (cat) in THF at 70 °C, 24 h (red asterisk = Hydrolysis product of Et ₃ SiH; HS = Hydrosilylation; DS = Dehydrogenative Silylation)..	24
Figure S29. GCMS trace for 1-octene, Et ₃ SiH, C1-Rh (cat) in CDCl ₃ at 70 °C, 24 h (red asterisk = Hydrolysis product of Et ₃ SiH; HS = Hydrosilylation; DS = Dehydrogenative Silylation)..	24
Figure S30. GCMS trace for 1-octene, Et ₃ SiH, C1-Ir (cat) in toluene at 80 °C, 24h.	25
Figure S31. GCMS trace for 1-octene, Et ₃ SiH, [Rh(CO)Cl(PPh ₃) ₂] (cat) in toluene at 80 °C, 24 h (red asterisk = Hydrolysis product of Et ₃ SiH; HS = Hydrosilylation; DS = Dehydrogenative Silylation)... ..	25
Figure S33. GCMS trace for 1-octene, Et ₃ SiH, Sn1-Rh (cat) in toluene at 80 °C, 24 h. (red asterisk = Hydrolysis product of Et ₃ SiH; HS = Hydrosilylation; DS = Dehydrogenative Silylation).	26
Figure S34. GCMS trace for 1-octene, Et ₃ SiH, Sn1-Ir (cat) in toluene at 80 °C, 24 h.	27
Figure S35. GCMS trace for 1-octene, PhMe ₂ SiH, C1-Rh (cat) in toluene at 80 °C, 24 h.	27
Figure S36. GCMS trace for 1-octene, PhMe ₂ SiH, Sn1-Rh (cat) in toluene at 80 °C, 24 h.	28
Figure S37. GCMS trace for 1-pentene, Et ₃ SiH, C1-Rh (cat) in toluene at 80 °C, 24 h (red asterisk = Hydrolysis product of Et ₃ SiH; HS = Hydrosilylation; DS = Dehydrogenative Silylation).	28
.....	28
Figure S38. GCMS trace for 1-hexene, Et ₃ SiH, C1-Rh (cat) in toluene at 80 °C, 24 h (red asterisk = Hydrolysis product of Et ₃ SiH; HS = Hydrosilylation; DS = Dehydrogenative Silylation).	29
Figure S39. GCMS trace for 1-heptene, Et ₃ SiH, C1-Rh (cat) in toluene at 80 °C, 24 h (red asterisk = Hydrolysis product of Et ₃ SiH; HS = Hydrosilylation; DS = Dehydrogenative Silylation).	29
Figure S40. GCMS trace for 4-phenyl-1-butene, Et ₃ SiH, C1-Rh (cat) in toluene at 25 °C, 24 h (\$ = Hydrolysis product of Et ₃ SiH; # = Unreacted alkene; * = Isomerised/hydrogenated alkenes).	30
Figure S41. GCMS trace for allylpentafluorobenzene, Et ₃ SiH, C1-Rh (cat) in toluene at 25 °C, 24 h (\$ = Hydrolysis product of Et ₃ SiH; # = Unreacted alkene; * = Isomerised/hydrogenated alkenes; % = Unidentified product).	30
Figure S42. GCMS trace for 4-chloro-styrene, Et ₃ SiH, C1-Rh (cat) in toluene at 80 °C, 24 h (# = Unreacted alkene; * = Isomerised/hydrogenated alkenes; % = Unidentified product).	31
Figure S43. GCMS trace for α-methyl heptene, Et ₃ SiH, C1-Rh (cat) in toluene at 80 °C, 24 h.	31
Figure S44. GCMS trace for 1-hexene, PhMe ₂ SiH, C1-Rh (cat) in toluene at 80 °C, 24 h.....	32
Figure S45. GCMS trace for 1-heptene, PhMe ₂ SiH, C1-Rh (cat) in toluene at 80 °C, 24 h.....	32
Figure S46. GCMS trace for 1-octene, PhMe ₂ SiH, C1-Rh (cat) in toluene at 80 °C, 24 h.....	33

Figure S47. GCMS trace for 4-phenyl-1-butene, PhMe ₂ SiH, C1-Rh (cat) in toluene at 80 °C, 24 h.	33
Figure S48. GCMS trace for 3-phenoxypropene, PhMe ₂ SiH, C1-Rh (cat) in toluene at 80 °C, 24 h.	34
Figure S49. GCMS trace for methyl eugenol, PhMe ₂ SiH, C1-Rh (cat) in toluene at 80 °C, 24 h. ...	34
Figure S50. GCMS trace for methyl eugenol, Ph(Me) ₂ SiH, Sn1-Rh (cat) in toluene at 80 °C, 24 h.	35
Figure S51. GCMS trace for 1-octene, (EtO) ₃ SiH, C1-Rh (cat) in toluene at 80 °C, 24 h.	35
Figure S52. GCMS trace for Cycle-I: 1-octene, Et ₃ SiH, C1-Rh (cat) in toluene at 80 °C, 24 h.	36
Figure S53. GCMS trace for Cycle-II: 1-octene, Et ₃ SiH, C1-Rh (cat) in toluene at 80 °C, 24 h.	36
Figure S54. GCMS trace for Cycle-III: 1-octene, Et ₃ SiH, C1-Rh (cat) in toluene at 80 °C, 24 h.	37
Figure S55. ¹ H NMR (300 MHz) spectrum of the C1 in CDCl ₃ .	38
Figure S56. ¹³ C{ ¹ H} NMR (75 MHz) spectrum of the C1 in CDCl ₃ .	38
Figure S57. ³¹ P{ ¹ H} NMR (122 MHz) spectrum of the C1 in CDCl ₃ .	39
Figure S58. HR-ESI-TOFMS (positive mode) of C1.	39
Supplementary Tables	40
Table S1. Detail optimization for the catalytic conversion of 1-octene.	40
Table S2. Substrate cope of the hydrosilylation reaction using C1-Rh MOF as a catalyst.	41
Table S3. Crystal data, data collection and refinement parameters for the structure of C1-Rh.	42
Table S4. Crystal data, data collection and refinement parameters for the structure of C1-Ir.	43

Experimental

General information for synthesis

Experiments were carried under inert conditions using standard Schlenk techniques or a glove box as appropriate. Tetrahydrofuran (THF) was dispensed from an MBRAUN Solvent Purification System, deoxygenated by bubbling nitrogen for 20 min, and stored over 3 Å molecular sieves prior to use. Chloroform-*d* (CDCl₃), benzene-*d*₆ (C₆D₆) and toluene-*d*₈ (C₇D₈) solvents were used as received without any purification and those were stored over 4 Å molecular sieves prior to use. J. Young flasks (10 mL), vials (20 mL), and stir bars for reactions were oven-dried overnight before experiments.

General information for material characterization

¹H (300 or 400 MHz), ³¹P (162 MHz), and ¹³C{¹H} (101 MHz) NMR spectra were run at 298 K on either a Bruker 300 MHz AVA or on a Jeol 400 spectrometer. The chemical shifts (δ, ppm) for ¹H and ¹³C{¹H} NMR spectra are given relative to solvent signals whereas an external reference standard was used for ³¹P (85% H₃PO₄) NMR spectra. The NMR data are given as: chemical shift, multiplicity (s = singlet, d = doublet, t = triplet, q = quartet, m = multiplet, br = broad), coupling constants (Hz) and integration. The single-crystal X-ray diffraction (SCXRD) data was collected on a Bruker APEX II Ultra CCD diffractometer which was equipped with a microfocus rotation anode using MoKα radiation (λ = 0.7107 Å) at 100 K. Structures were solved and refined using Full-matrix least-squares with a suite of programs SHELXT and SHELXL (Sheldrick, G. M., *Acta Cryst. Sec. A*, **2008**, 64, 112) compiled in OLEX2 (Dolomanov, O. V.; Bourhis, L. J.; Gildea, R. J.; Howard, J. A. K.; and Puschmann, H. *J. Appl. Crystallogr.*, **2009**, 42, 339-341). Crystal data, data collection and refinement parameters are summarized in Table S3-S4. Powder X-ray diffraction (PXRD) data were collected using a Bruker D8 ADVANCE diffractometer LynxEye XET detector running at 40 kV, 40 mA for Cu Kα (λ = 1.5418 Å), with a scan speed of 1 sec/step, a step size of 0.1° in 2θ, and a 2θ range of 5-50° at room temperature. PXRD samples were loaded on a silicon sample holder. Sample holders used were zero-background Si plates (p-type, B-doped) from MTI Corp. Well-type sample holders (depth = 0.5 mm) were used. The tetra-phosphine linker **C1** was prepared by following a modified literature protocol (Yang, Y.; Beele, B. and Blümel, J., *J. Am. Chem. Soc.*, **2008**, 130, 3771-3773). All other reagents were purchased commercially and used as received.

Synthesis of C1

The tetra-phosphine linker **C1** was prepared by following a modified literature protocol (Yang, Y.; Beele, B. and Blümel, J., *J. Am. Chem. Soc.*, **2008**, 130, 3771-3773). The reaction was conducted employing standard Schlenk line techniques, utilizing a 250 mL Schlenk flask

equipped with a stir bar. *n*-BuLi (3.78 mL, 9.46 mmol, 2.5 M in hexane, 4.01 equiv.) was added dropwise to a THF (125 mL) solution of tetrakis(4-bromophenyl)methane (1.5 g, 2.36 mmol, 1.0 equiv.) at -78 °C. After stirring the mixture for 2.5 h at -78 °C, chlorodiphenylphosphane (1.74 mL, 9.46 mmol, 4.01 equiv.) was added, and the mixture was gradually warmed to room temperature and stirred overnight. The reaction was quenched with degassed MeOH followed by dry loading onto a flash column chromatography column. DCM/hexane eluent was used, yielding **C1** as a white solid (1.47 g, 59.0% yield). ¹H NMR (300 MHz, CDCl₃): δ 7.40 – 7.23 (m, 40H), 7.21 - 7.07 (m, 16H). ¹³C NMR (75 MHz, CDCl₃): δ 146.6, 137.1 (d, *J* = 10.1 Hz), 135.1 (d, *J* = 10.2 Hz), 133.9 (d, *J* = 19.5 Hz), 132.9 (d, *J* = 19.1 Hz), 131.3 (d, *J* = 7.0 Hz), 128.9 (s), 128.6 (d, *J* = 7.2 Hz), 64.7. ³¹P{¹H} NMR (122 MHz, CDCl₃): δ -6.62 (s, 1 P). ESI-HRMS(+) *m/z* calculated for: [C₇₃H₅₇OP₄+H]⁺: 1073.33; found: 1073.3354.

Synthesis of **C1-Rh** single crystals

Initial addition of reagents was carried out in a N₂ filled glove box whilst subsequent purification and work-up was carried out under ambient conditions. In a 10 mL round-bottom J-Young flask with a teflon tap adaptor, [RhCl(CO)(PPh₃)₂] (0.019 g, 0.028 mmol, 2.0 equiv.) and **C1** (0.015 g, 0.014 mmol, 1.0 equiv.) were added. Dry, degassed THF (2.0 mL) was then transferred into the flask and swirled to produce a clear, yellow solution. The flask was sealed and removed from the glove box. The flask was placed into a preheated oil bath at 80 °C for 7 d. Yellow crystals appeared after 7 d which were suitable for SCXRD. The resulting crystals were collected, centrifuged, and washed with THF (5×1 mL) followed by drying to afford **C1-Rh** (8.0 mg, 41%).

Scaled synthesis of **C1-Rh**

Initial addition of reagents was carried out in a N₂ filled glove box whilst subsequent purification and work-up was carried out under ambient conditions. In a 20 mL scintillation vial with a poly(ethylene) lined urea cone cap, [RhCl(CO)(PPh₃)₂] (0.057 g, 0.084 mmol, 2.0 equiv.) and **C1** (0.045 g, 0.042 mmol, 1.0 equiv.) were added. Dry, degassed THF (5.0 mL) was transferred, and the vial was swirled to dissolve solids, producing a clear, yellow solution. The vial was sealed with Teflon tape and black electrical wire tape before removal from the glove box. The vial was placed in a preheated oil bath at 80 °C for 7 d. The resulting yellow crystals were collected, centrifuged, and washed with THF (5×2 mL) followed by drying to afford **C1-Rh** (26.0 mg, 44%). The resulting microcrystals were not suitable for SCXRD, but PXRD analysis of the bulk sample showed similar microcrystalline phases to be identical to the **C1-Rh** single crystal synthesis described above.

Synthesis of C1-Rh with modulator

Initial addition of reagents was carried out in a N₂ filled glove box whilst subsequent purification and work-up was performed under ambient conditions. In a 10 mL round-bottom J-Young flask with a Teflon cap adaptor, [RhCl(CO)(PPh₃)₂] (0.019 g, 0.028 mmol, 2.0 equiv.) and tri(*o*-tolyl)phosphine (0.017 g, 0.056 mmol, 4.0 equiv.) were added and dissolved in dry, degassed THF (1.5 mL). The flask was swirled to dissolve solids, affording a clear, yellow solution. A dry, degassed THF (1.5 mL) solution of **C1** (0.015 g, 0.014 mmol, 1.0 equiv.) was then transferred into the flask. The solution remained clear and yellow. The flask was sealed and removed from the glove box. The flask was placed in a preheated oil bath at 80 °C for 48h. The resulting yellow crystals were collected, centrifuged, and washed with THF (5×2 mL) followed by drying to afford **C1-Rh** (15.0 mg, 77%). The resulting microcrystals were not suitable for SCXRD, but PXRD analysis of the bulk sample showed similar microcrystalline phases that were identical to the **C1-Rh** single crystal synthesis described above.

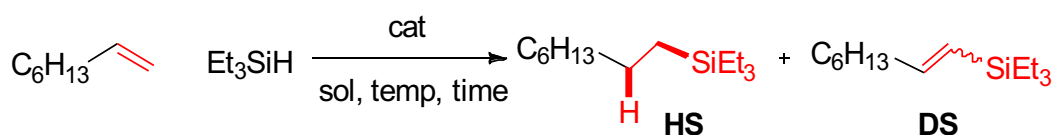
Synthesis of C1-Ir single crystals

To a 10 mL J. Young flask, [Ir(CO)Cl(PPh₃)₂] (0.022 g, 0.028 mmol) and the **C1** linker (0.015 g, 0.014 mmol) were added. The flask was then placed under Ar before the solids were dissolved in 2 mL of dry and degassed THF with swirling to give a clear, yellow solution. The flask was then placed in a pre-heated oil bath at 100 °C for 6 d. The resulting mixture was removed from heat and the supernatant was decanted. Single crystals suitable for SCXRD were suspended in 0.5 mL THF and removed from the reaction vessel.

Synthesis of C1-Ir with modulator

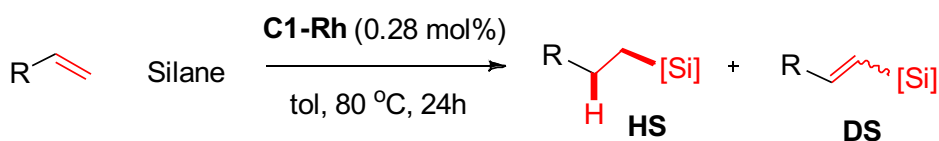
To a 10 mL J. Young flask, tri(*o*-tolyl)phosphine (0.017 g, 0.056 mmol), [Ir(CO)Cl(PPh₃)₂] (0.022 g, 0.028 mmol), and the **C1** linker (0.015 g, 0.014 mmol) were added. The flask was then placed under Ar before the mixture was dissolved in 2 mL of dry and degassed THF with swirling to give a clear, yellow solution. The flask was then placed in a pre-heated oil bath at 100 °C for 45 h. The resulting mixture was removed from heat, sonicated, and transferred to a 1.5 mL Eppendorf tube. The mixture was centrifuged and the supernatant was removed and washed with THF (2×1.0 mL). The resulting solid was dried under Ar flow to afford **C1-Ir** as a bright yellow solid (14 mg, 62% yield).

Optimization conditions for hydrosilylation of 1-Octene with Et₃SiH



Initial addition of reagents was carried out in a N₂ filled glove box whilst subsequent manipulation was performed under ambient conditions. To a 20 mL scintillation vial equipped with a poly(ethylene) lined urea cone cap and a stir bar, 1-octene (0.067 g, 0.6 mmol, 2.0 equiv.) and triethylsilane, Et₃SiH (0.035 g, 0.3 mmol, 1.0 equiv.) were added. Catalyst (0.28 mol%) in a designated solvent (1.0 mL) was transferred to the reaction vial. The vial was sealed with both Teflon tape and black electrical wire tape and then removed from the glove box. The vial was placed in a preheated oil bath at 80 °C for 24 h. The reaction yield and selectivity of the products were assessed by GCMS analysis with an internal *n*-dodecane standard. Formation of hydrogenative silylation (HS) and dehydrogenative silylation (DS) products was also confirmed by ¹H NMR analysis. A summary of the optimization of the reaction conditions is listed in Table S1.

Procedure for examining the scope of hydrosilylation with C1-Rh



Initial addition of reagents was carried out in a N₂ filled glove box whilst subsequent manipulation was performed under ambient conditions. To a 20 mL scintillation vial equipped with a poly(ethylene) lined urea cone cap and a stir bar, an alkene (0.6 mmol, 2.0 equiv.) and a silane (0.3 mmol, 1.0 equiv.) were added. **C1-Rh** MOF (1.9 mg, 0.28 mol%) was suspended in toluene (1.0 mL) and transferred to the reaction vial. The vial was sealed with Teflon tape and black electrical wire tape before removal from the glove box. The vial was placed in a preheated oil bath at 80 °C for 24 h. The reaction yields and selectivity of the products were assessed by GCMS analysis with an internal *n*-dodecane standard. Products were also confirmed by ¹H NMR analysis. A summary of the scope for hydrosilylation reactions is listed in Table S2.

Filter Test of C1-Rh LVMOF for hydrosilylation of 1-Octene with Et₃SiH

Initial addition of reagents was carried out in a N₂ filled glove box whilst subsequent manipulation was performed under ambient conditions. To a 20 mL scintillation vial equipped with a poly(ethylene) lined urea cone cap and a stir bar, 1-octene (0.067 g, 0.6 mmol, 2.0 equiv.) and Et₃SiH (0.035 g, 0.3 mmol, 1.0 equiv.) were added. **C1-Rh** (1.9 mg, 0.28 mol%) was suspended in toluene (1.0 mL) and transferred to the reaction vial. Also, *n*-dodecane was added to the reaction as an internal standard. The vial was sealed with Teflon tape and black electrical wire tape before removing from the glove box. After 30 min heating at 80 °C, the catalyst **C1-Rh** was removed by filtration using a syringe filter. The filtrate was isolated, and all volatiles were removed under reduced pressure. The oily residue was analysed by Inductively Coupled Plasma Mass Spectrometry (ICP-MS). ICP-MS analysis confirmed negligible dissolution of rhodium species under hydrosilylation conditions, indicating the catalyst remains largely intact during the reaction.

Recyclability of C1-Rh for hydrosilylation of 1-Octene with Et₃SiH

Initial addition of reagents was carried out in a N₂ filled glove box whilst subsequent manipulation was performed under ambient conditions. In a 20 mL scintillation vial equipped with a poly(ethylene) lined urea cone cap and a stir bar, 1-octene (0.067 g, 0.6 mmol, 2.0 equiv.) and Et₃SiH (0.035 g, 0.3 mmol, 1.0 equiv.) were added. **C1-Rh** LVMOF (1.9 mg, 0.28 mol%) was suspended in toluene (1.0 mL) and was transferred to the reaction vial. The vial was sealed with Teflon tape and black electrical wire tape before removal from the glove box. The vial was placed in a preheated oil bath at 80 °C for 24 h. After each run, GCMS yield assessment was performed against an internal *n*-dodecane standard. **C1-Rh** was recovered by centrifugation and was washed with degassed THF (5×1.0 mL). The recovered catalyst was then dried under vacuum in preparation for the next catalytic reaction. The decanted reaction mixture was filtered through two 0.22 µm syringe filters, and the volatiles were removed in vacuo prior to analysis by ICP-MS. The resulting yields were: Cycle I: 35±6% HS, 3±1% DS (*n*=2); Cycle II: 37±8% HS, 3±1% DS (*n*=2); Cycle III: 45±5% HS, 4±0% DS (*n*=2) (Figure S52-S54). ICP-MS analysis conducted after each reaction cycle confirmed that rhodium species underwent negligible dissolution under hydrosilylation conditions (Cycle I: 0.0046%; Cycle II: 0.00643%; Cycle III: 0.00744%).

Supplementary Figures

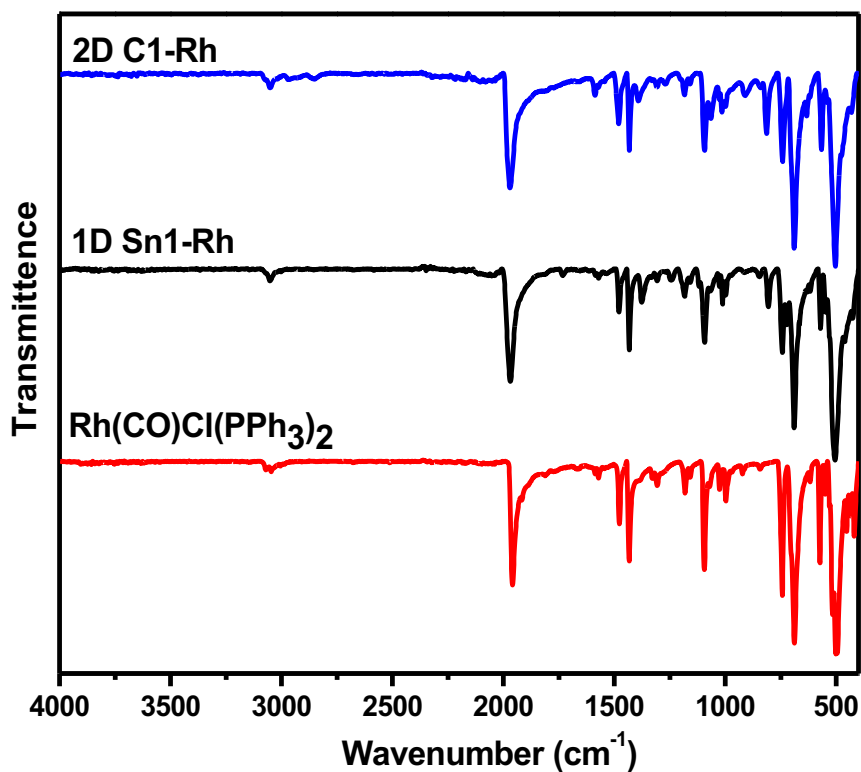


Figure S1. IR spectra of **C1-Rh** (blue), **Sn1-Rh** (black) and **[Rh(CO)Cl(PPh₃)₂]** (red).

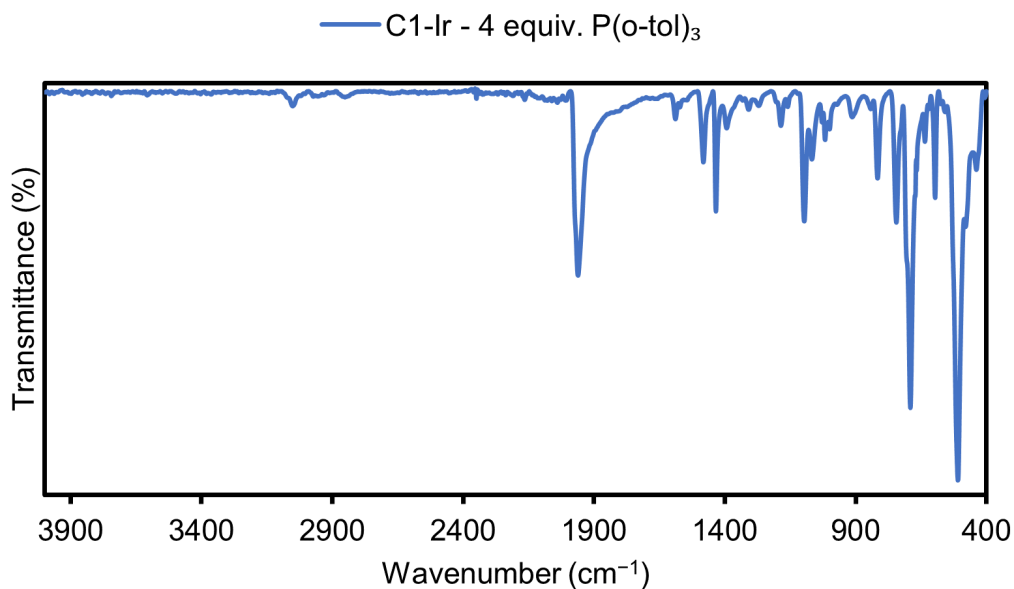


Figure S2. IR spectra of **C1-Ir** synthesized with the use of 4-equiv. tri(*o*-tolyl)phosphine.

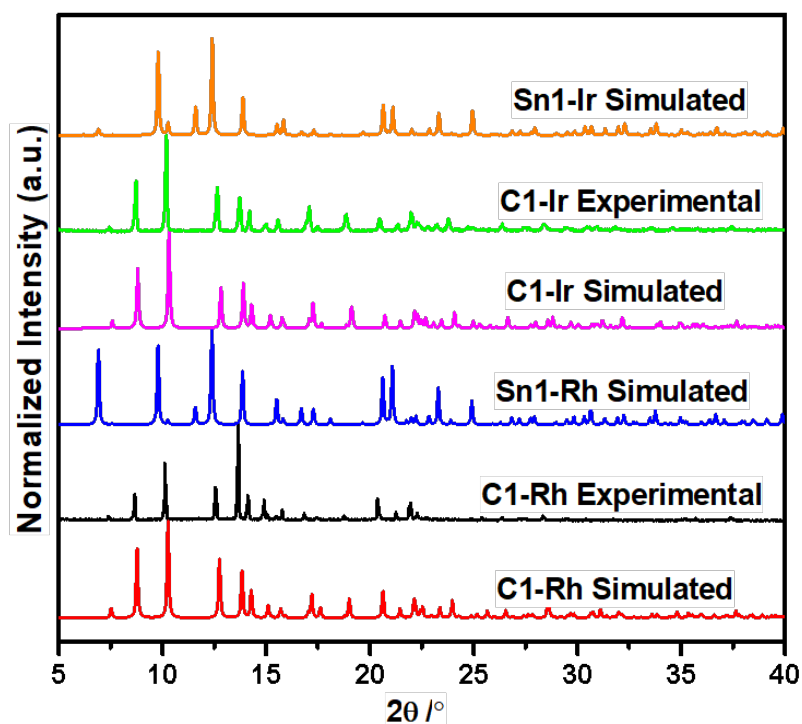


Figure S3. Simulated PXRD patterns of **C1-Rh** (red), **Sn1-Rh** (blue), **C1-Ir** (magenta) and **Sn1-Ir** (orange) and experimental PXRD pattern of **C1-Rh** (black) and **C1-Ir** (green).

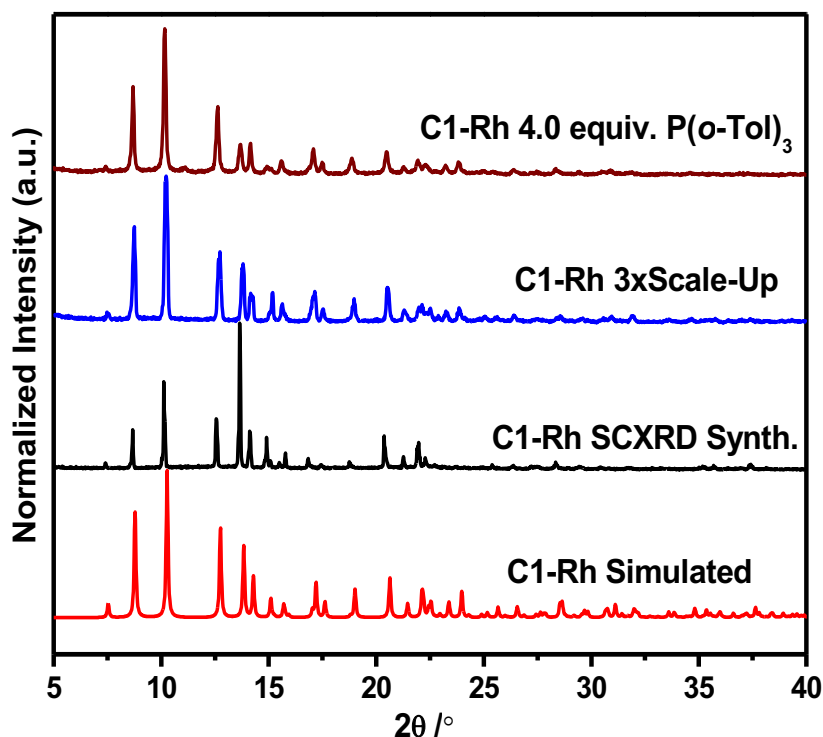


Figure S4. Simulated PXRD patterns of **C1-Rh** (red) and experimental PXRD pattern of **C1-Rh** SCXRD synthesis (black), **C1-Rh** scale-up synthesis (blue), **C1-Rh** 4.0 equiv. tri(*o*-tolyl)phosphine synthesis.

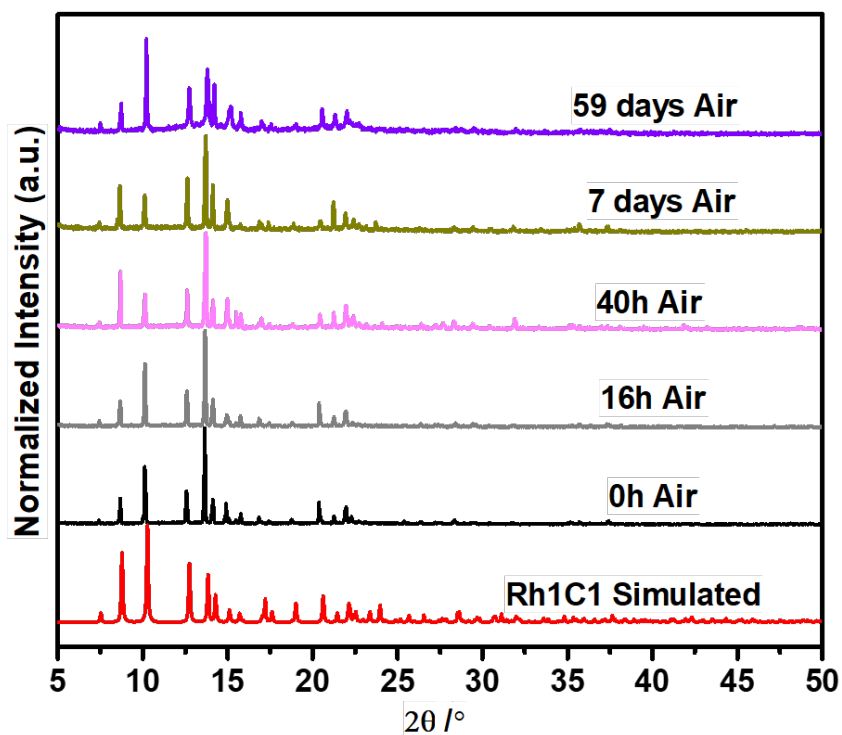


Figure S5. Air stability of **C1-Rh** as determined by PXRD after three months of exposure to ambient air.

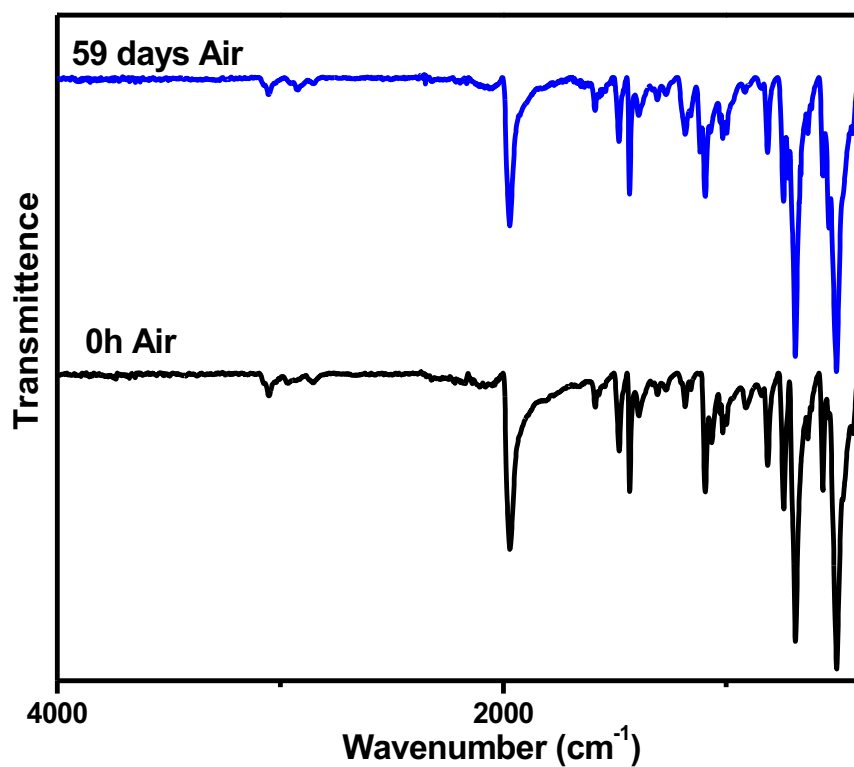


Figure S6. Air stability of **C1-Rh** as determined by IR analysis after three months of exposure to ambient air.

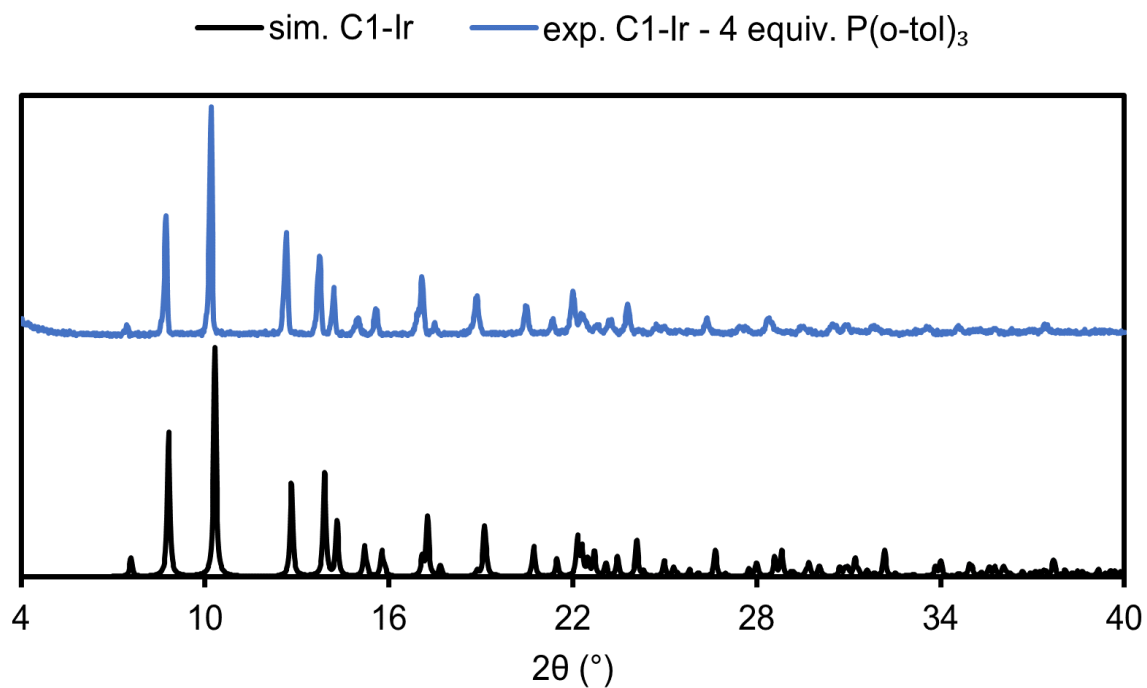


Figure S7. Simulated PXRD patterns of **C1-Ir** (pink) and experimental PXRD pattern of **C1-Rh** 4.0 equiv. tri(*o*-tolyl)phosphine synthesis (black).

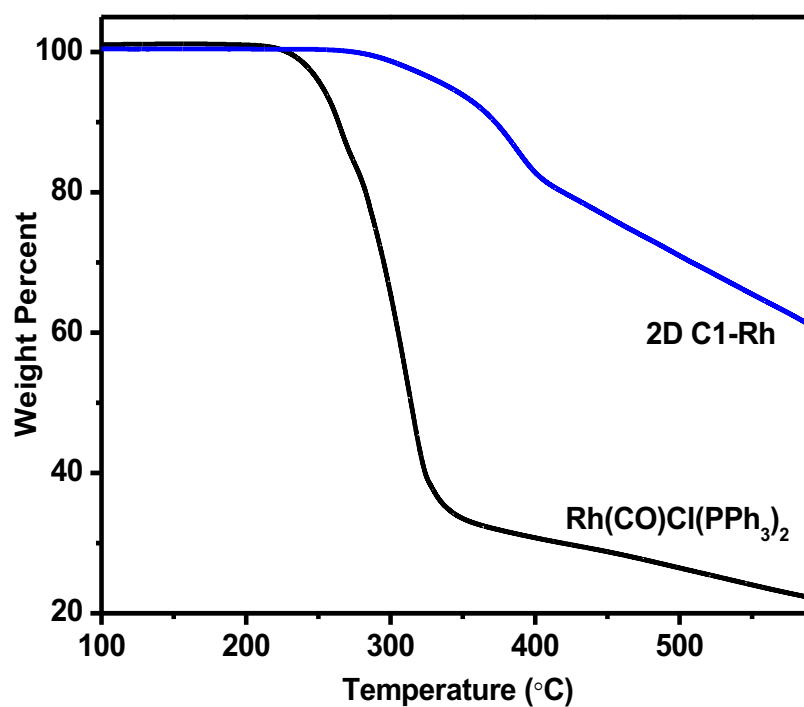


Figure S8. Thermogravimetric analysis of **C1-Rh** (blue) and $[\text{Rh}(\text{CO})\text{Cl}(\text{PPh}_3)_2]$ (black).

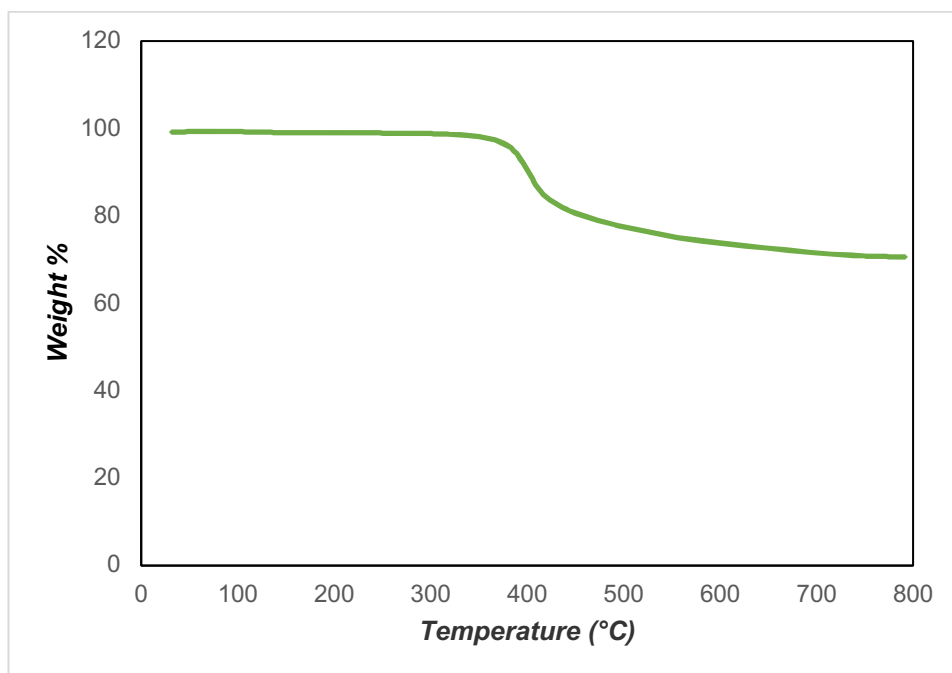


Figure S9. Thermogravimetric analysis of **C1-Ir**.

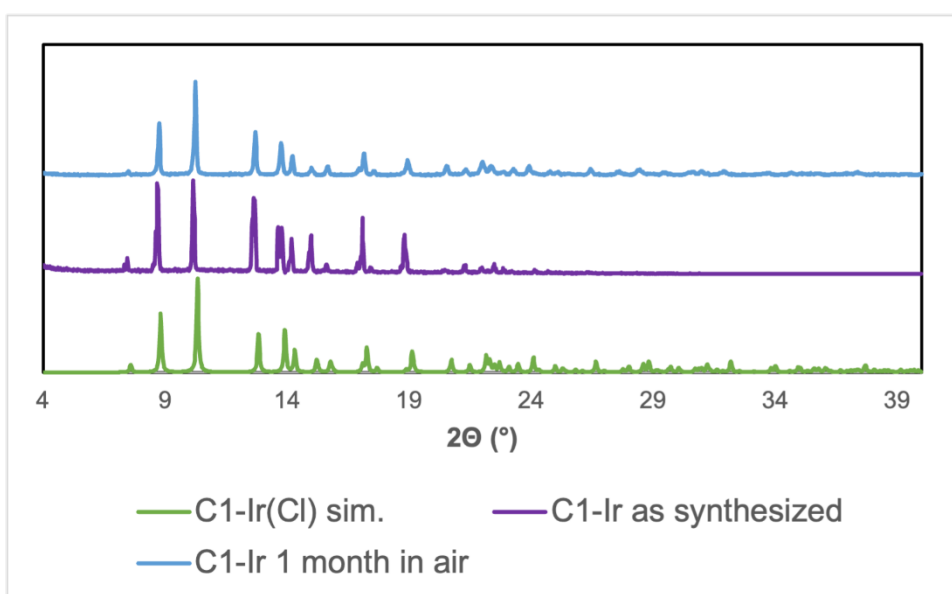


Figure S10. Air stability of **C1-Ir** as determined by PXRD after one month of exposure to ambient air.

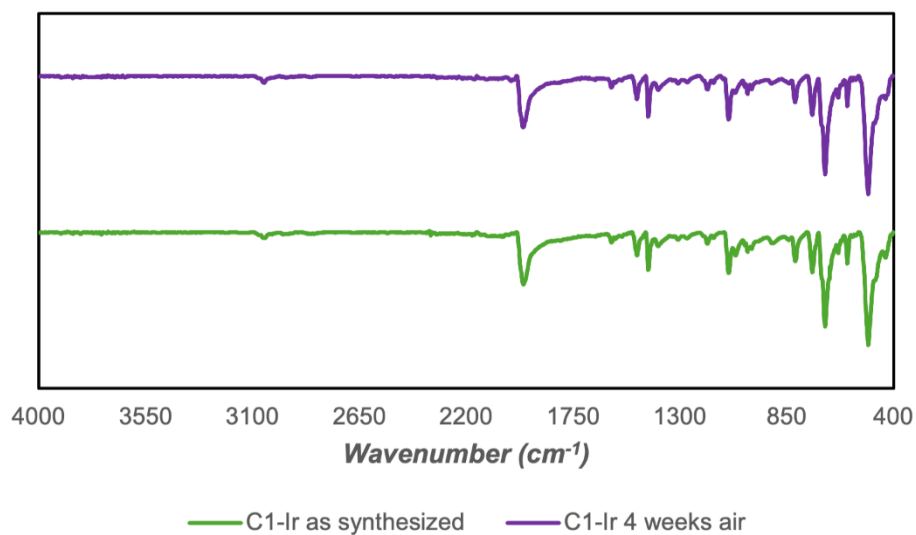


Figure S11. Air stability of **C1-Ir** as determined by IR analysis after one month of exposure to ambient air.

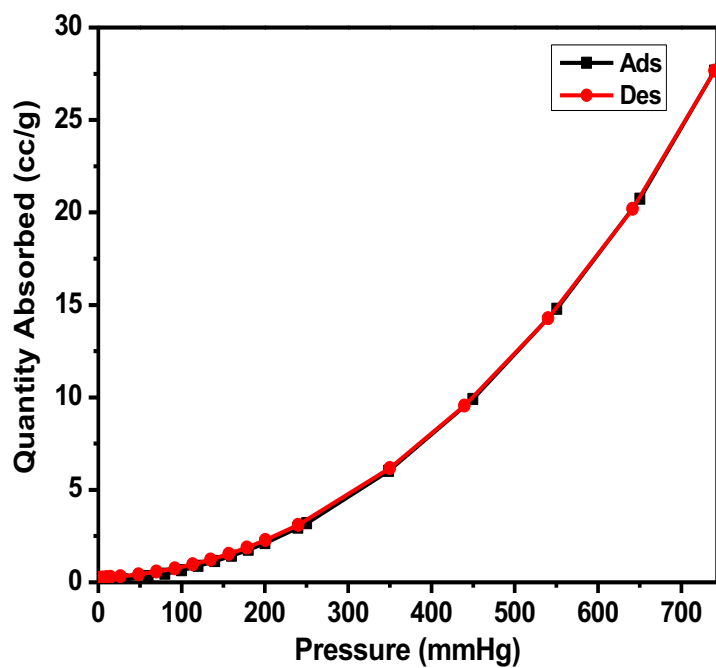


Figure S12. N₂ adsorption and desorption isotherm of **C1-Rh** at 77K.

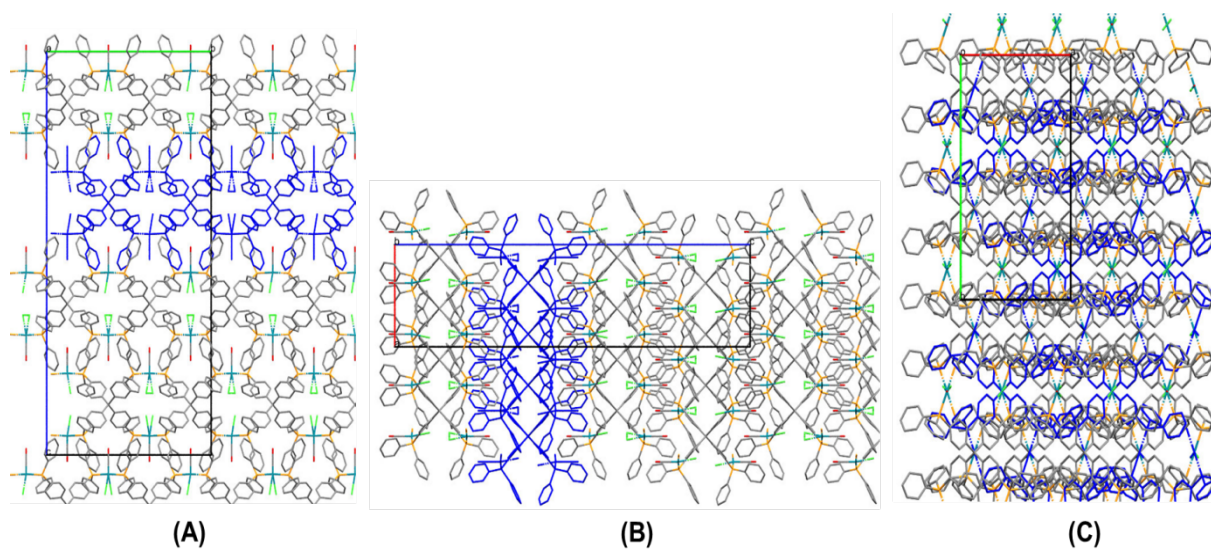


Figure S13. Wireframe images of **C1-Rh** extended structure viewed along (A) the crystallographic a-axis, (B) the b-axis, and (C) the c-axis.

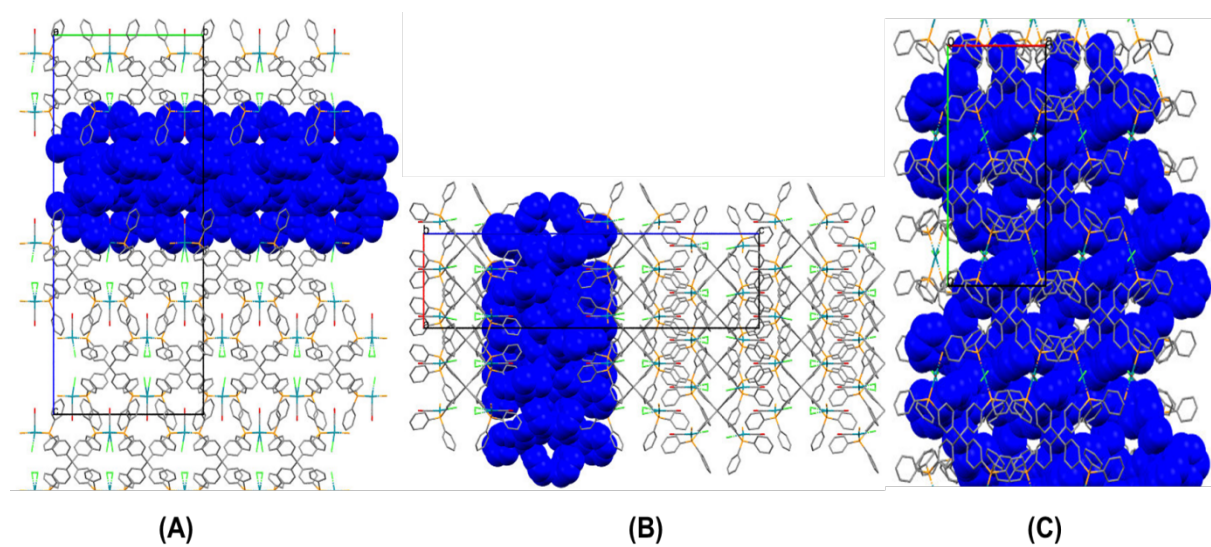


Figure S14. Space-filling images of **C1-Rh** extended structure viewed along (A) the crystallographic a-axis, (B) the b-axis, and (C) the c-axis.

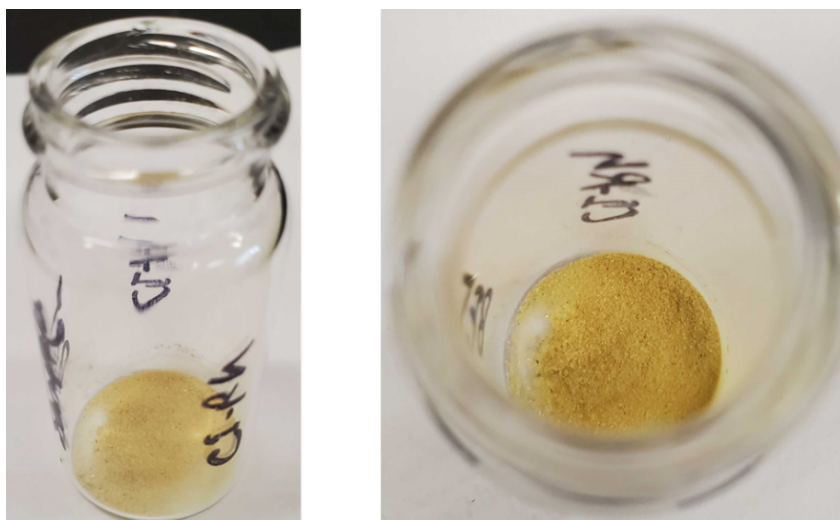


Figure S15. Images of dry and powdery sample of **C1-Rh** in a 20 mL vial with side view (*left*) and top view (*right*).

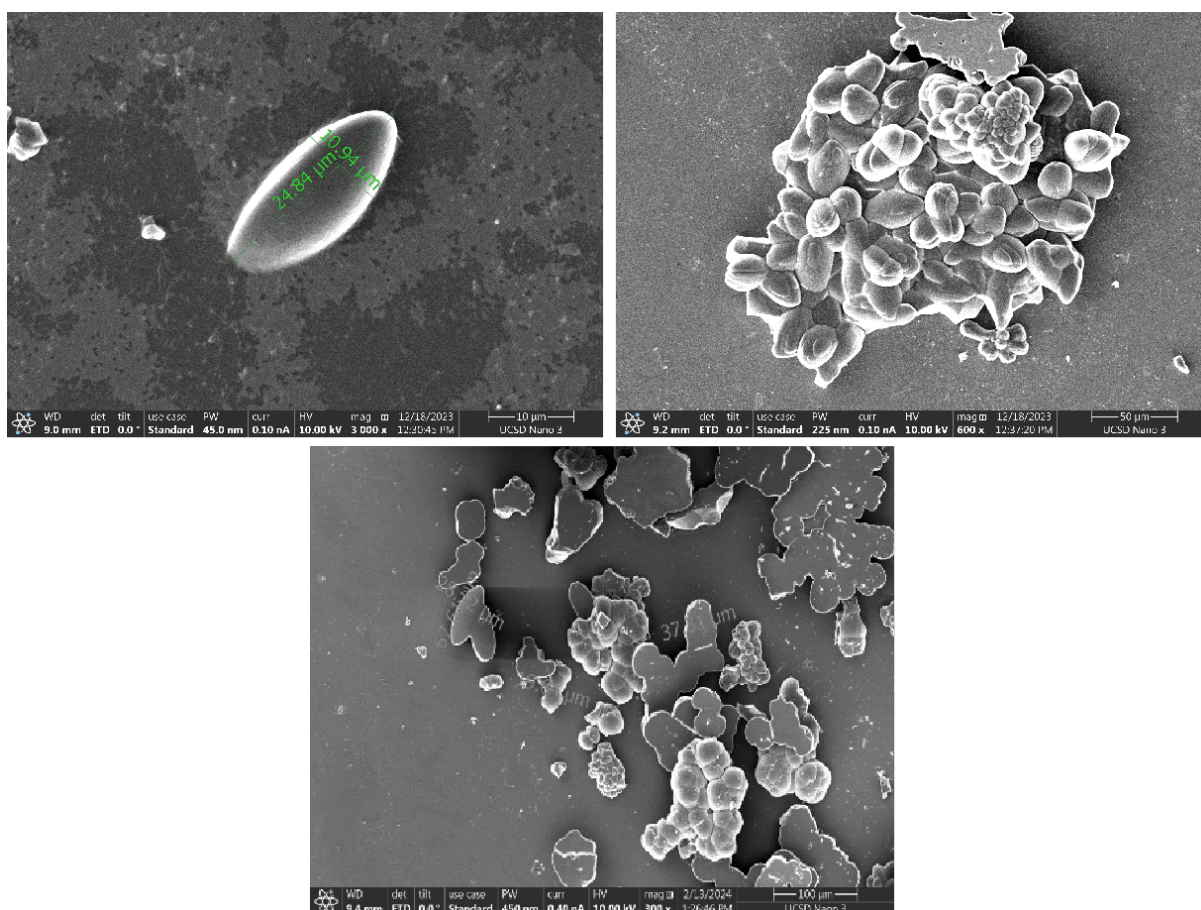


Figure S16. SEM images of **C1-Rh** synthesized without modulator in THF, 80 °C for 7 d.

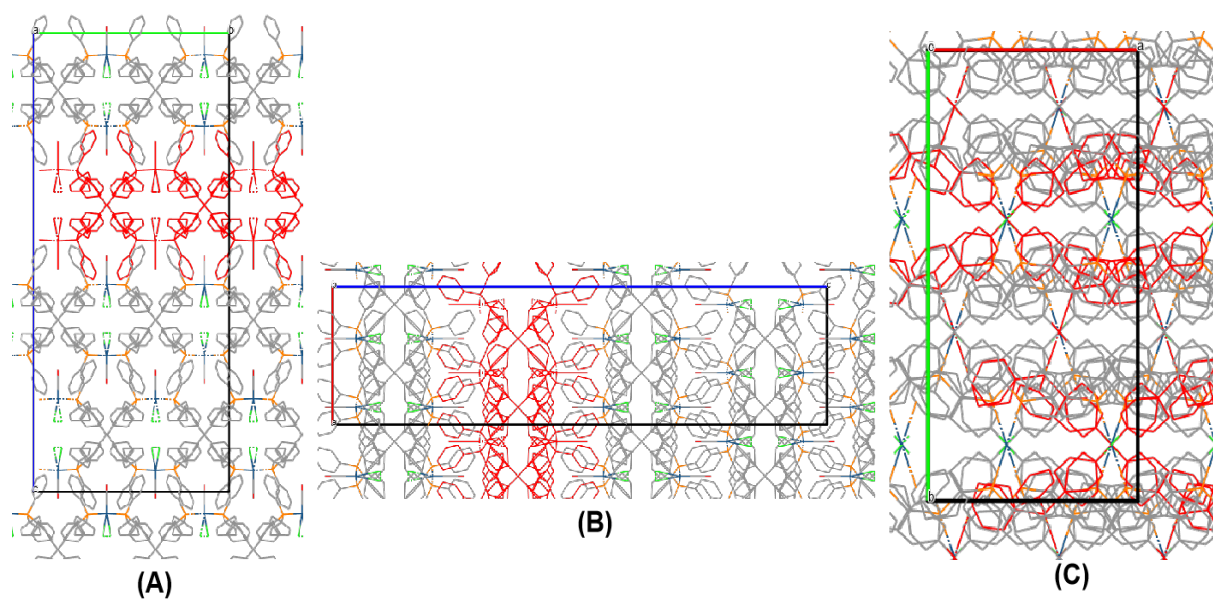


Figure S17. Wireframe images of **C1-Ir** extended structure viewed along (A) the crystallographic *a*-axis, (B) the *b*-axis, and (C) the *c*-axis.

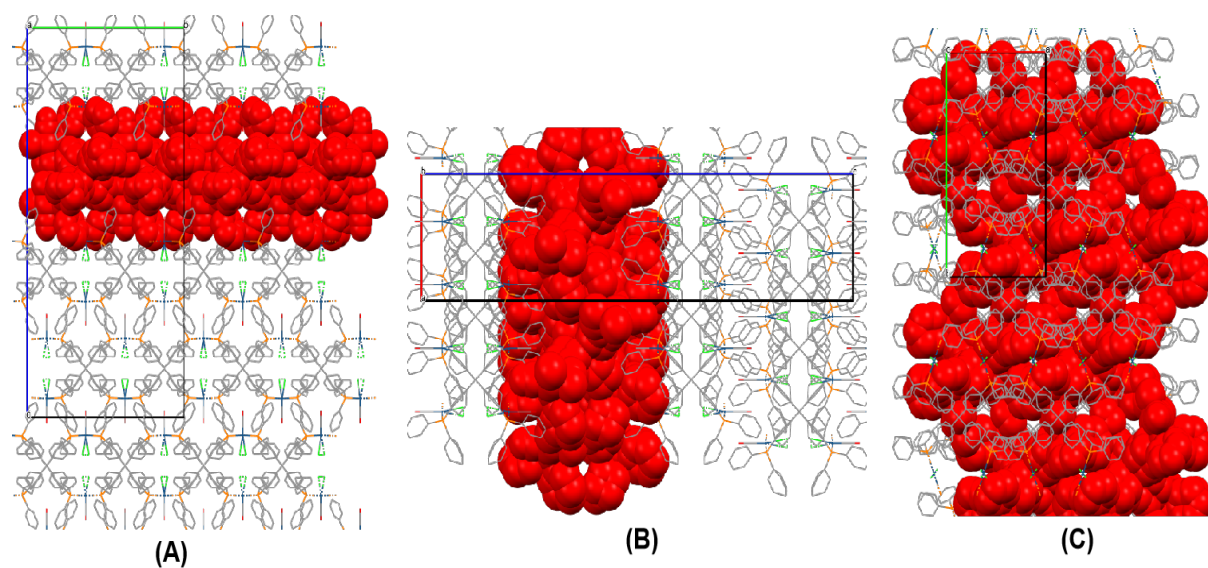


Figure S18. Spacefill images of **C1-Ir** extended structure viewed along (A) the crystallographic *a*-axis, (B) the *b*-axis, and (C) the *c*-axis.

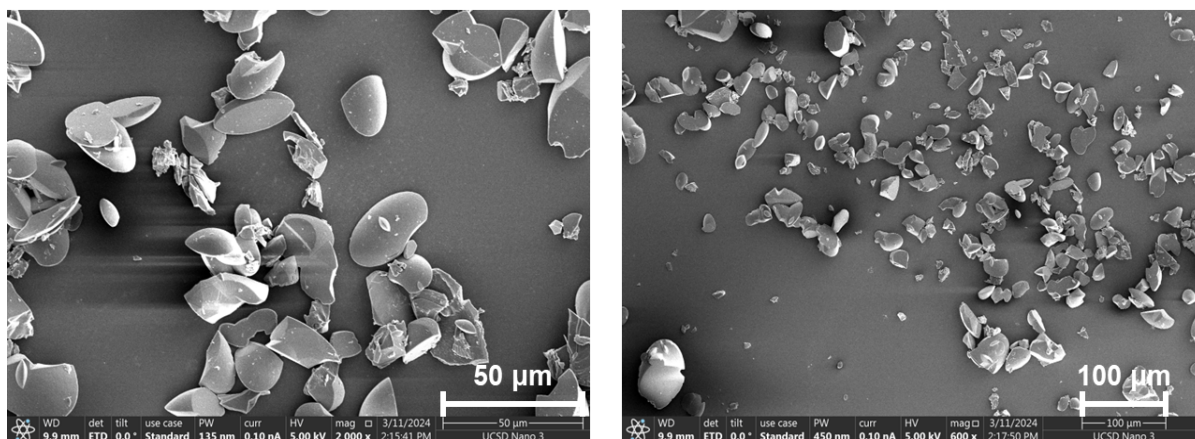


Figure S19. SEM images of **C1-Ir** synthesized without modulator in THF, 80 °C for 5 d.

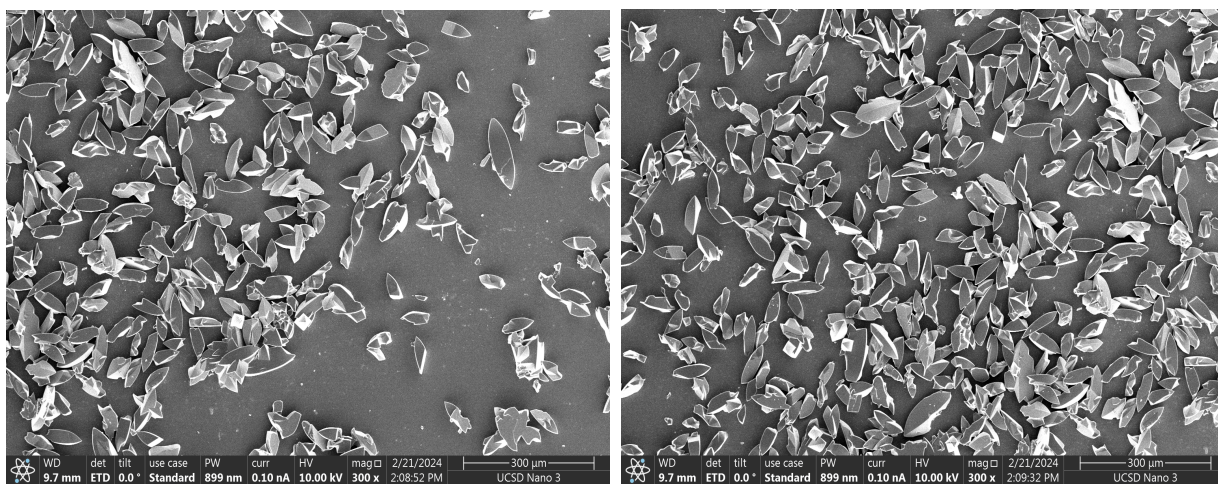


Figure S20. SEM images of **Sn1-Rh** synthesis adopted from *Angew. Chem. Int. Ed.* **2022**, 61, e202115454.

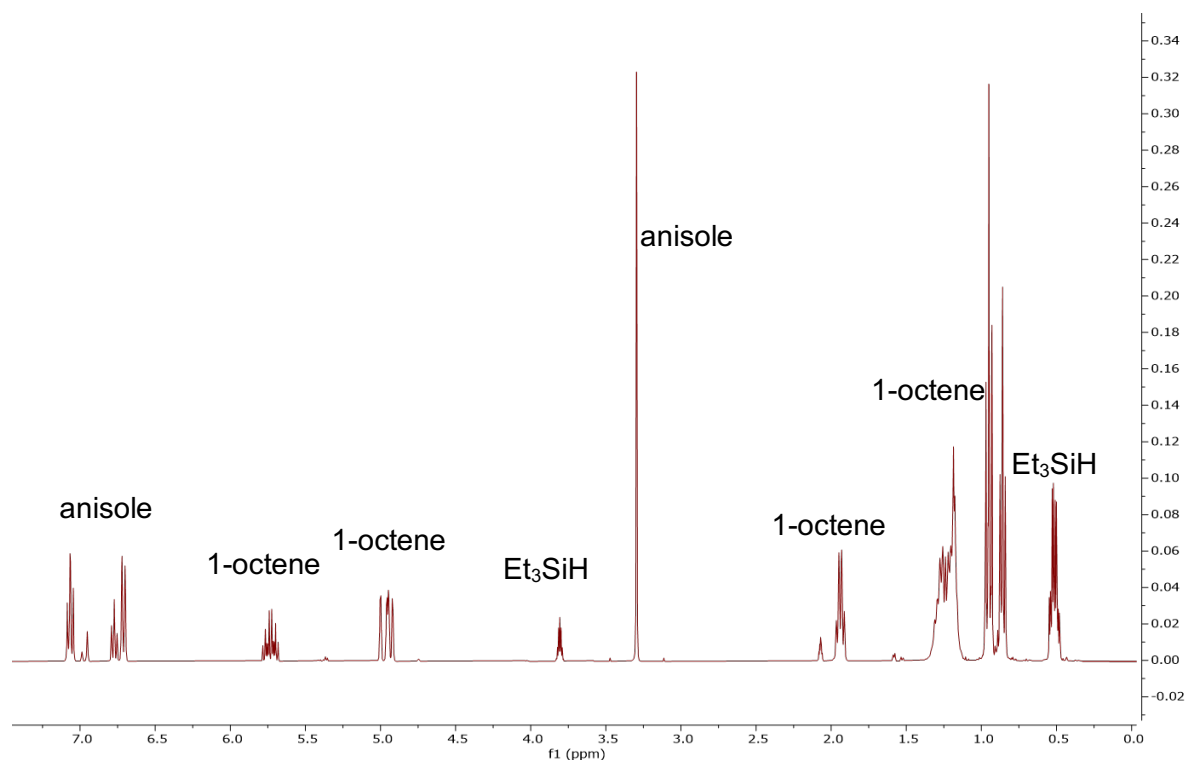


Figure S21. ^1H NMR spectrum of the crude mixture for the control reaction (1-octene, Et₃SiH) in d₈-toluene at 80 °C, 24 h (anisole as a reference standard).

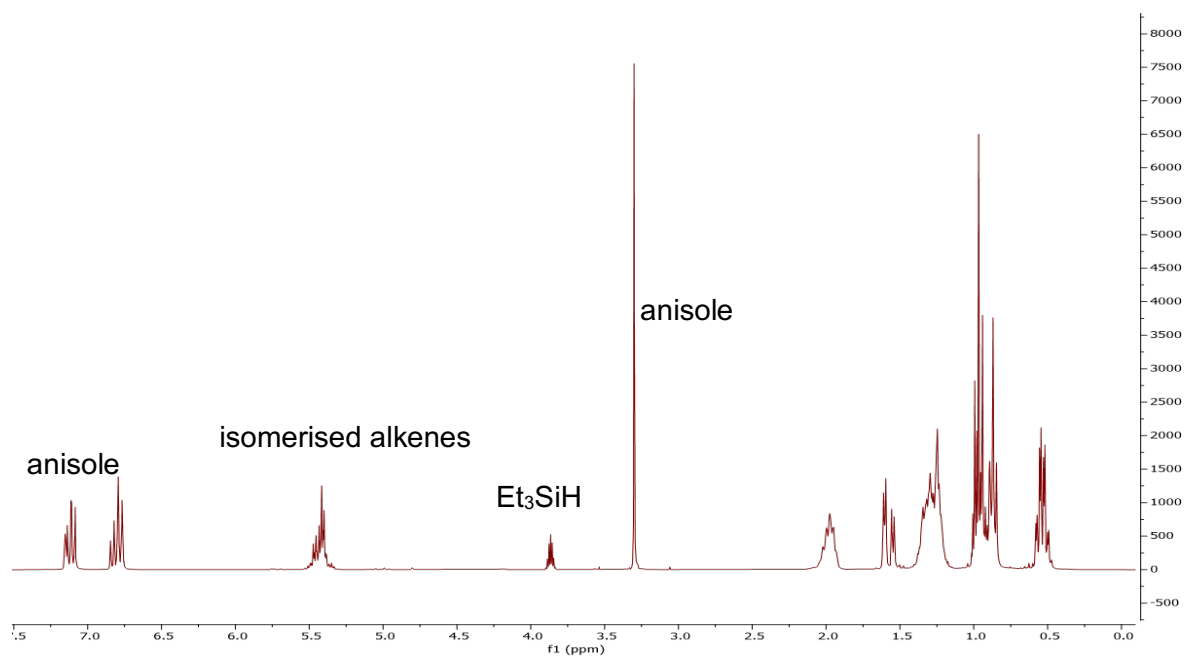


Figure S22. ^1H NMR spectrum of the crude mixture of 1-octene, Et₃SiH, **C1-Rh** (cat) in toluene at 80 °C, 24 h (anisole as reference standard).

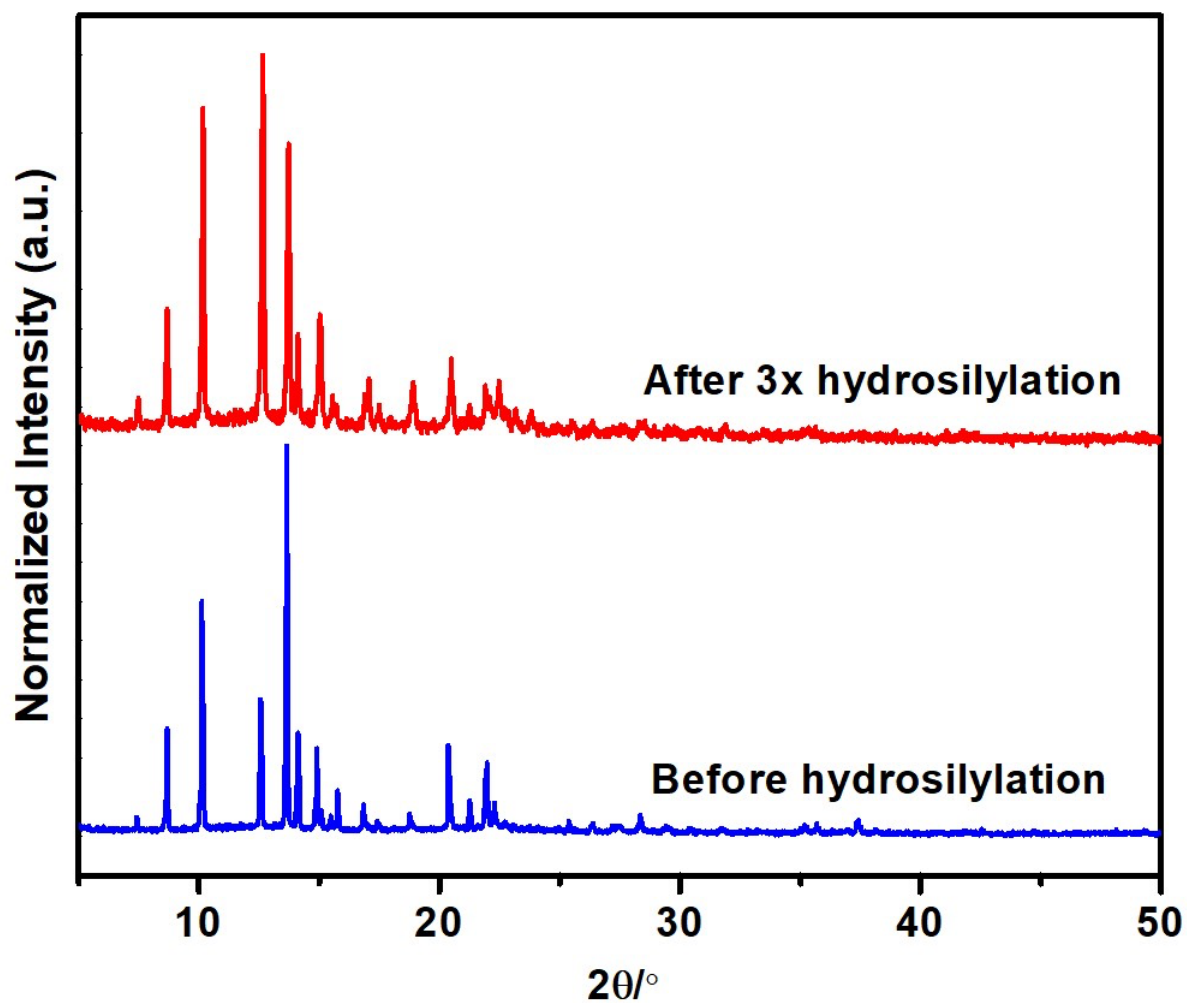


Figure S23. PXRD patterns of **C1-Rh** before hydrosilylation (blue) and after three rounds (3x) of hydrosilylation (red) of 1-octene with Et_3SiH at 80 °C for 24 h in toluene.

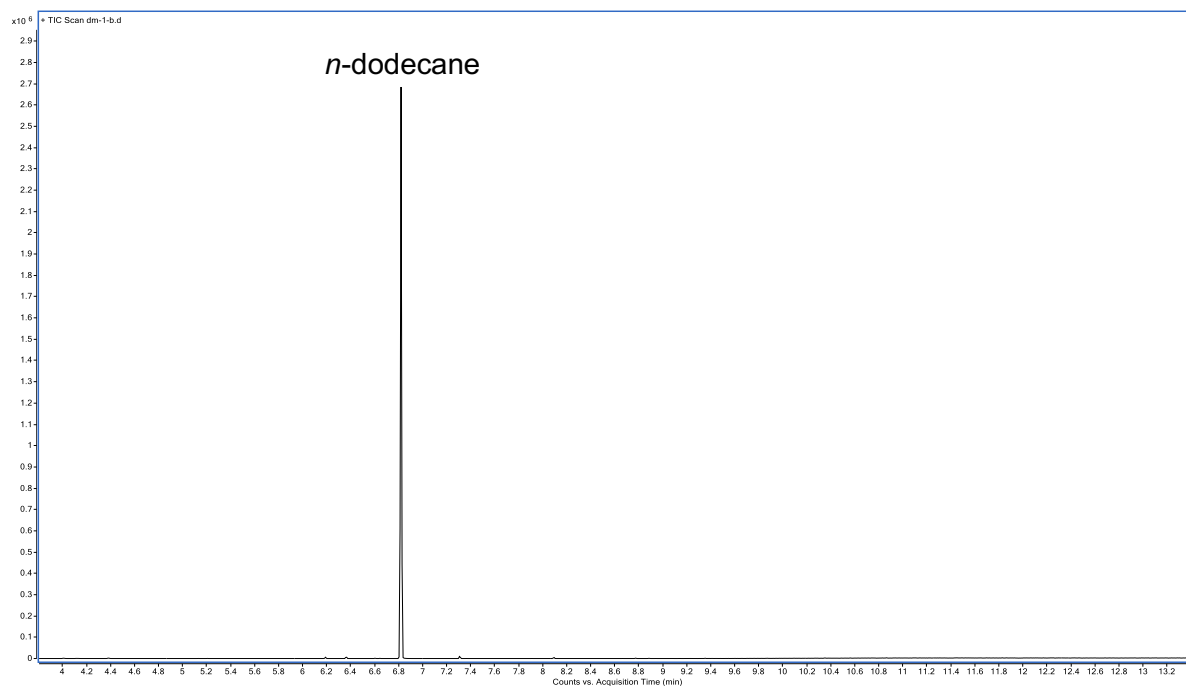


Figure S24. GCMS trace for the control of 1-octene and Et₃SiH in toluene at 80 °C, 24 h (*n*-dodecane internal standard).

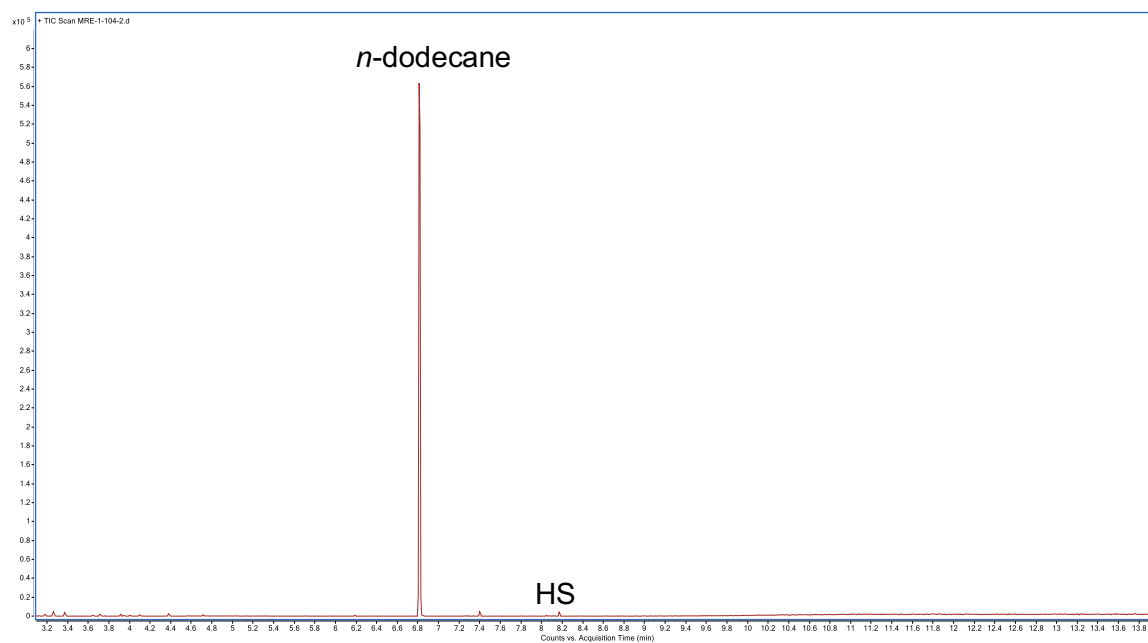


Figure S25. GCMS trace for 1-octene, Et₃SiH, Rh-C1 (cat) in toluene at 25 °C, 24 h.

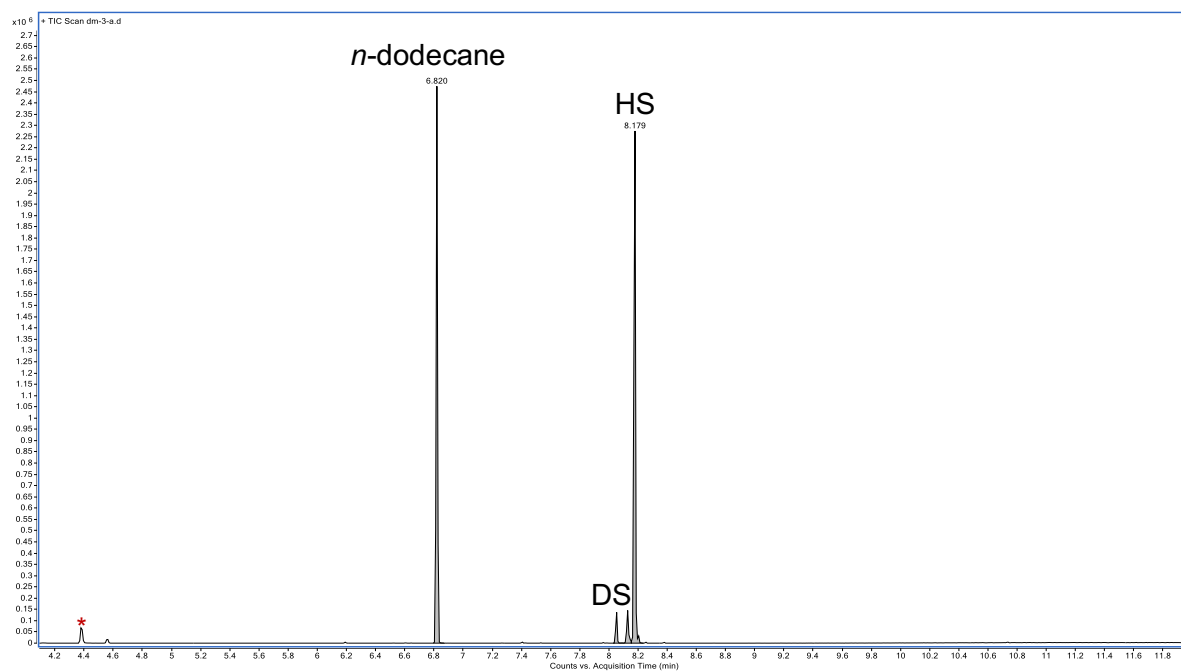


Figure S26. GCMS trace for 1-octene, Et₃SiH, **C1-Rh** (cat) in toluene at 80 °C, 24 h (red asterisk = Hydrolysis product of Et₃SiH; HS = Hydrosilylation; DS = Dehydrogenative Silylation).

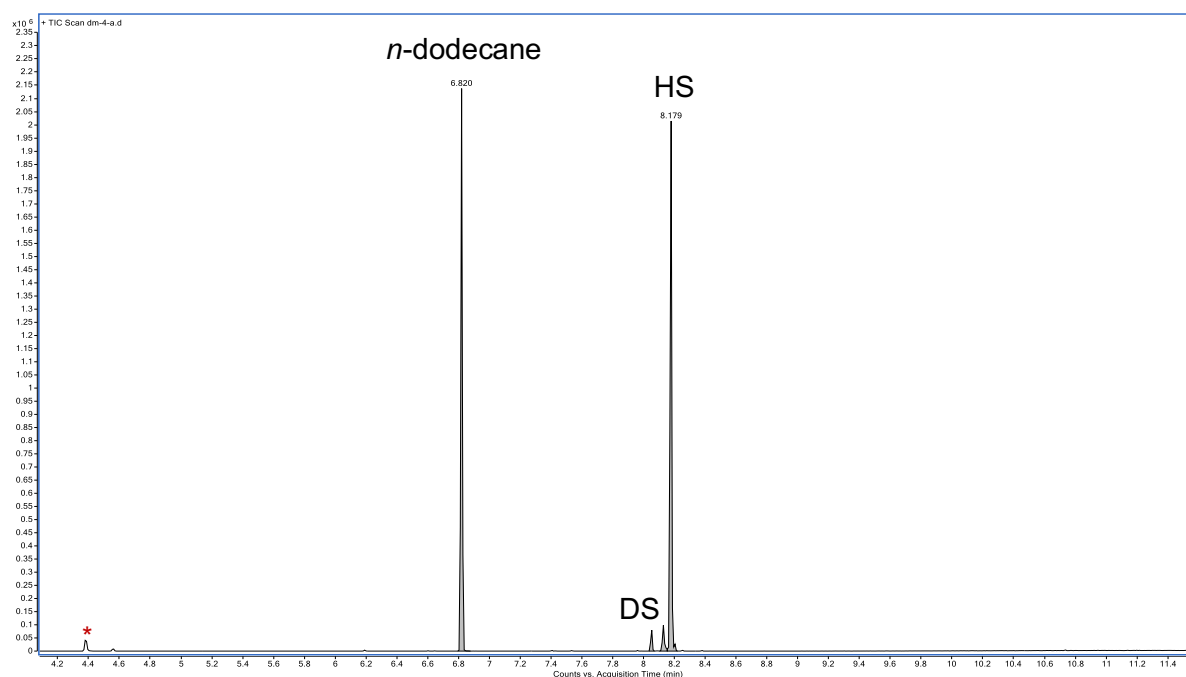


Figure S27. GCMS trace for 1-octene, Et₃SiH, **C1-Rh** (cat) in benzene at 80 °C, 24h (red asterisk = Hydrolysis product of Et₃SiH; HS = Hydrosilylation; DS = Dehydrogenative Silylation).

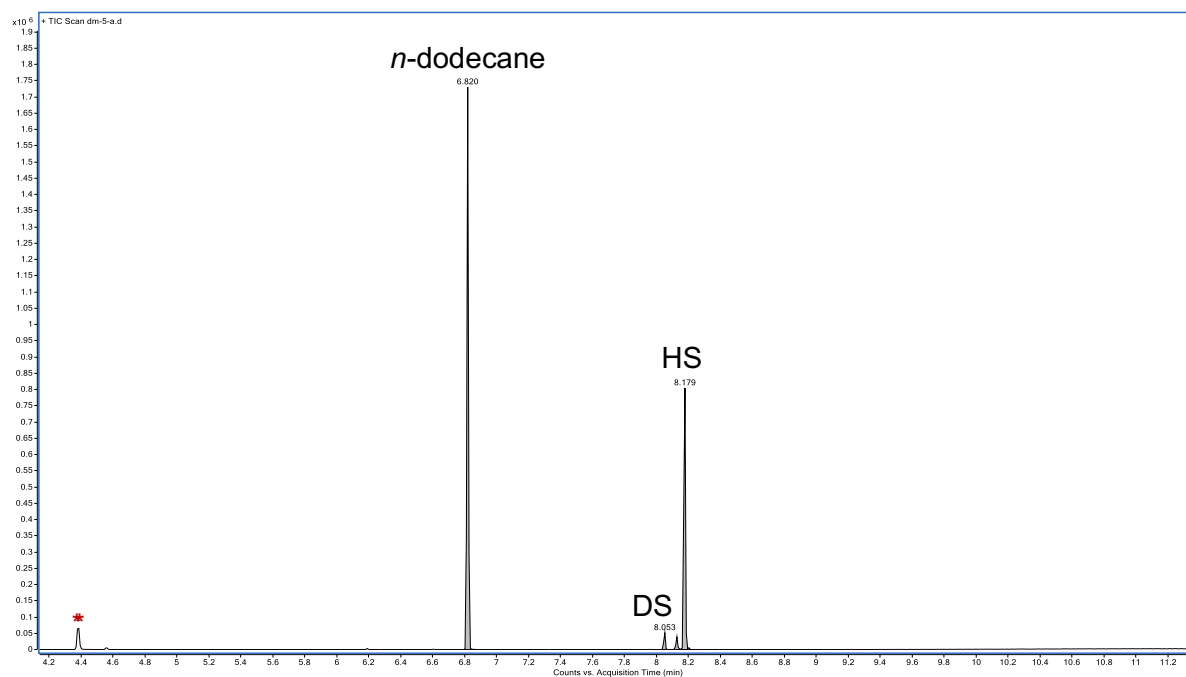


Figure S28. GCMS trace for 1-octene, Et₃SiH, **C1-Rh** (cat) in THF at 70 °C, 24 h (red asterisk = Hydrolysis product of Et₃SiH; HS = Hydrosilylation; DS = Dehydrogenative Silylation)..

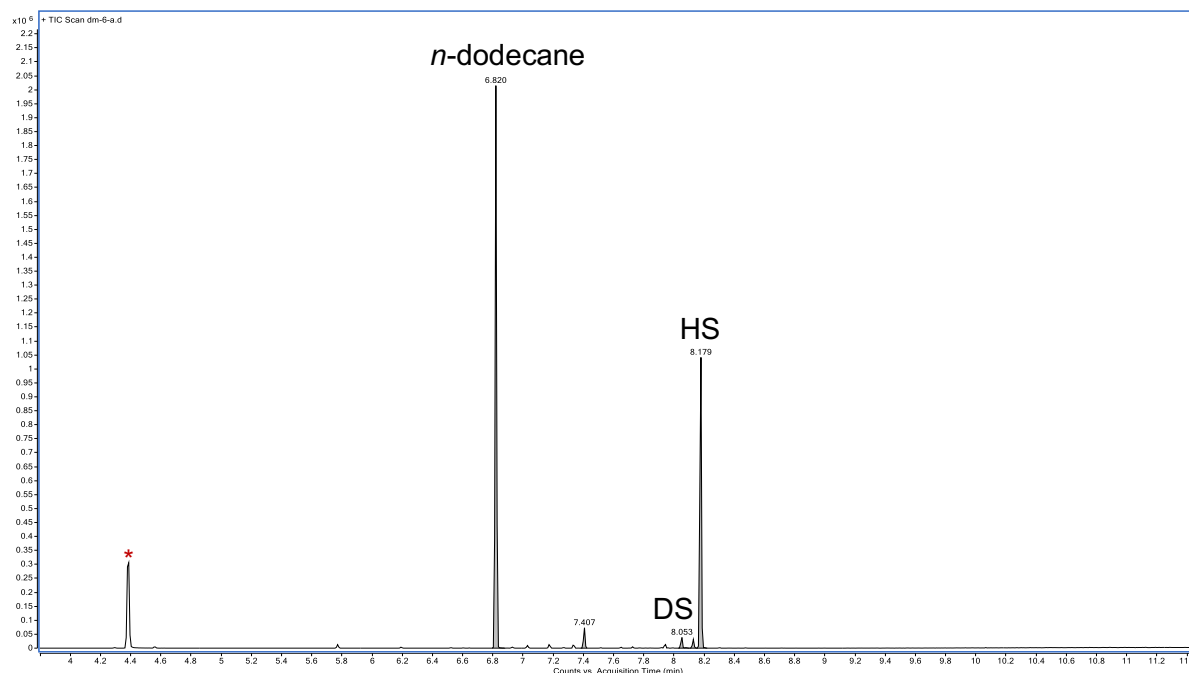


Figure S29. GCMS trace for 1-octene, Et₃SiH, **C1-Rh** (cat) in CDCl₃ at 70 °C, 24 h (red asterisk = Hydrolysis product of Et₃SiH; HS = Hydrosilylation; DS = Dehydrogenative Silylation)..

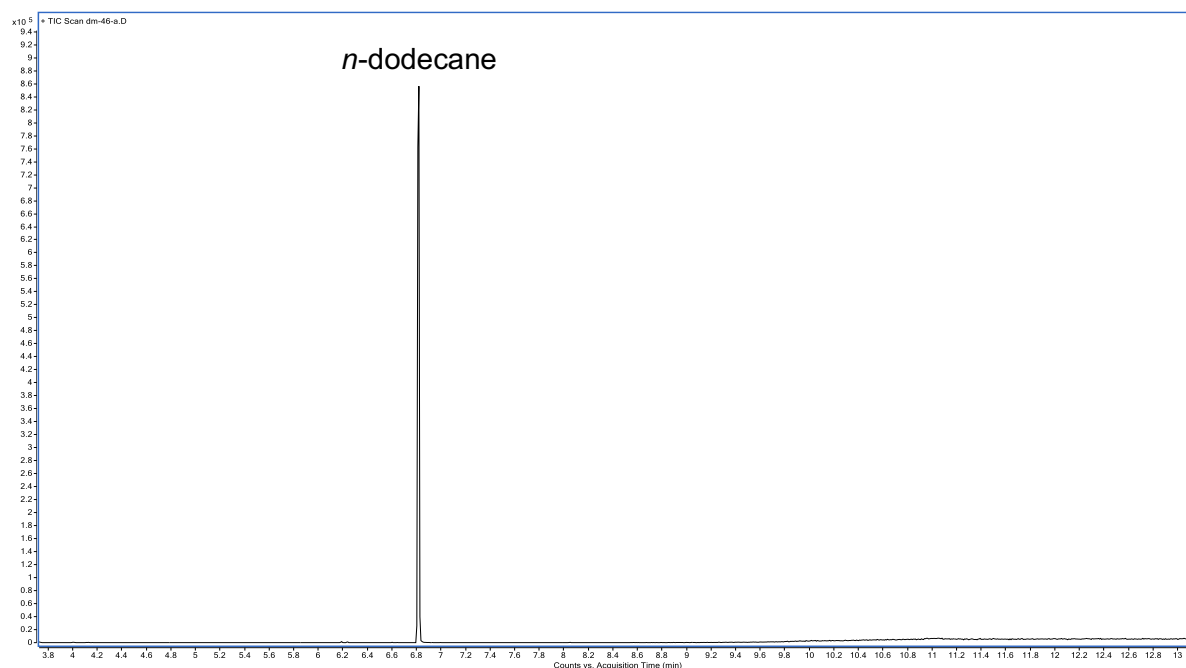


Figure S30. GCMS trace for 1-octene, Et_3SiH , **C1-Ir** (cat) in toluene at 80 °C, 24h.

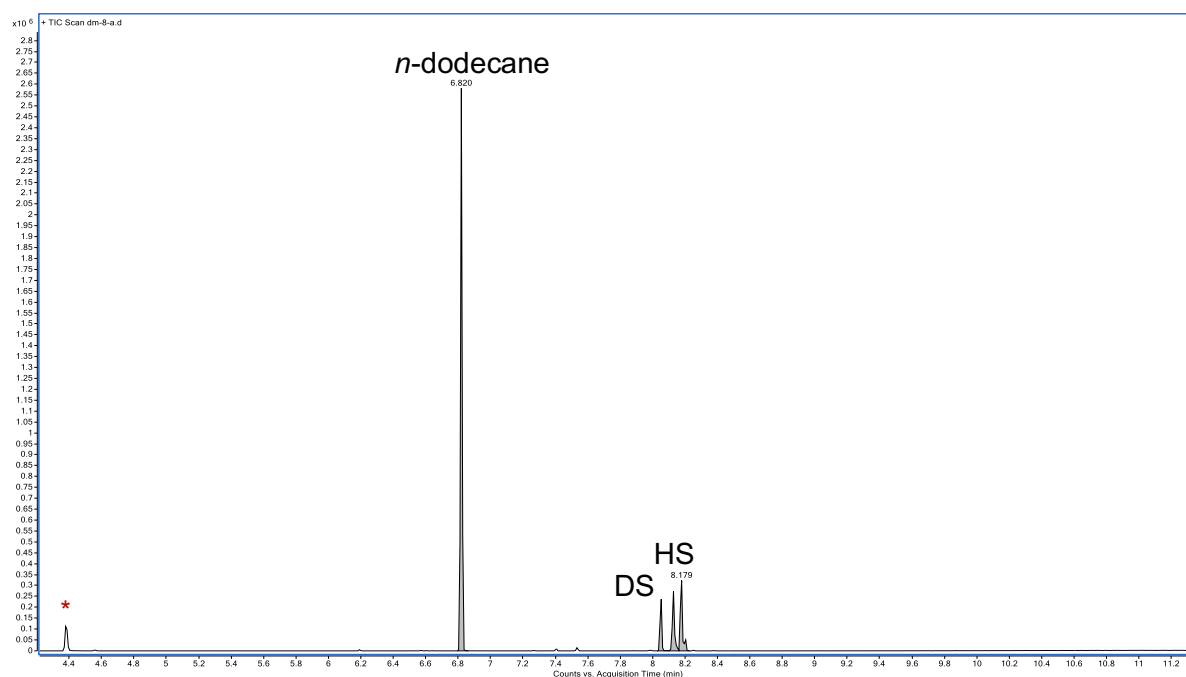


Figure S31. GCMS trace for 1-octene, Et_3SiH , $[\text{Rh}(\text{CO})\text{Cl}(\text{PPh}_3)_2]$ (cat) in toluene at 80 °C, 24 h (red asterisk = Hydrolysis product of Et_3SiH ; HS = Hydrosilylation; DS = Dehydrogenative Silylation).

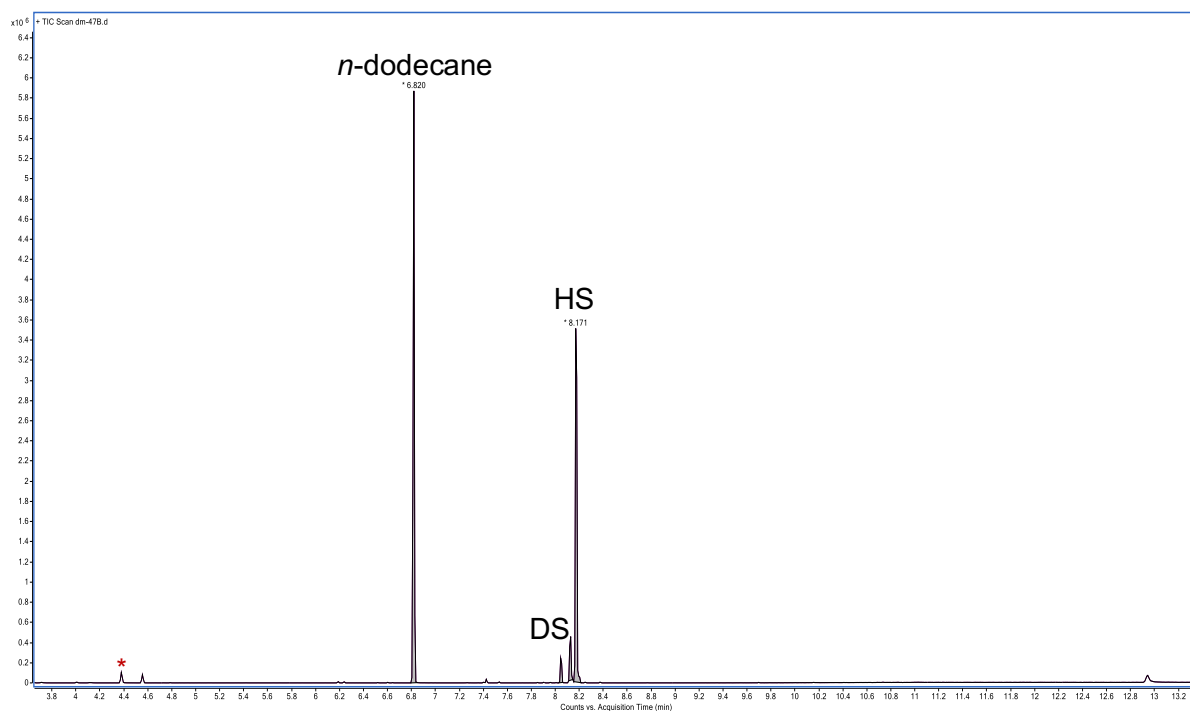


Figure S32. GCMS trace for 1-octene, Et₃SiH, [RhCl(PPh₃)₃] (cat) in toluene at 80 °C, 24h (red asterisk = Hydrolysis product of Et₃SiH; HS = Hydrosilylation; DS = Dehydrogenative Silylation).

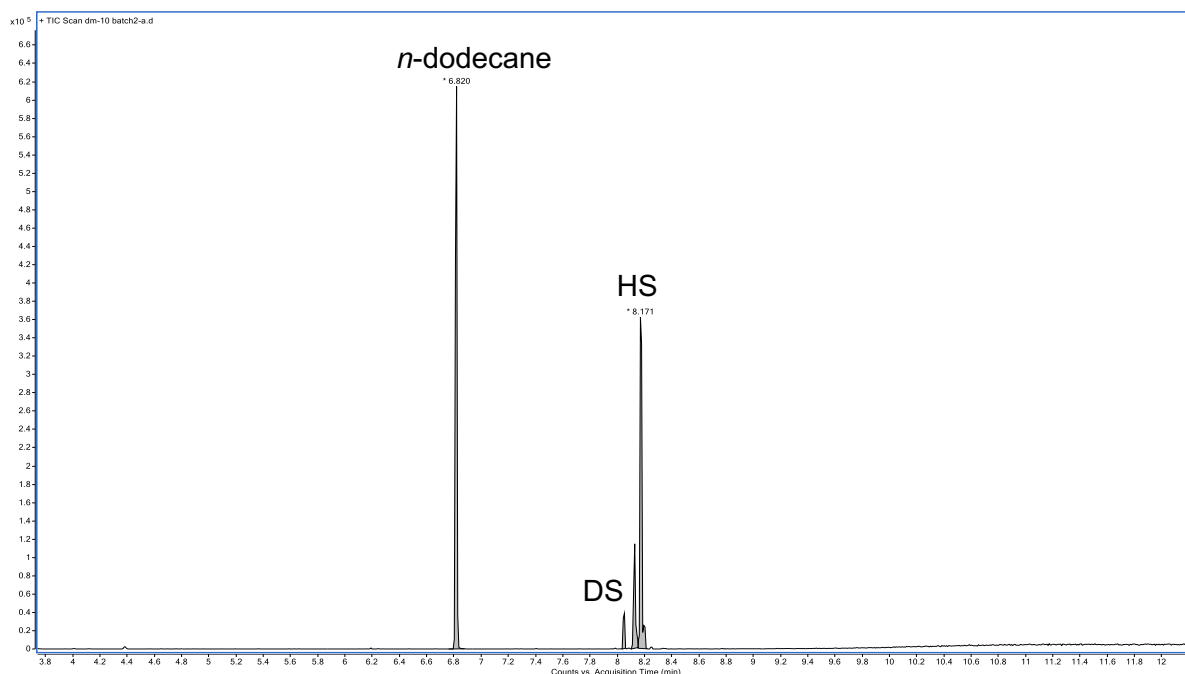


Figure S33. GCMS trace for 1-octene, Et₃SiH, Sn1-Rh (cat) in toluene at 80 °C, 24 h. (red asterisk = Hydrolysis product of Et₃SiH; HS = Hydrosilylation; DS = Dehydrogenative Silylation).

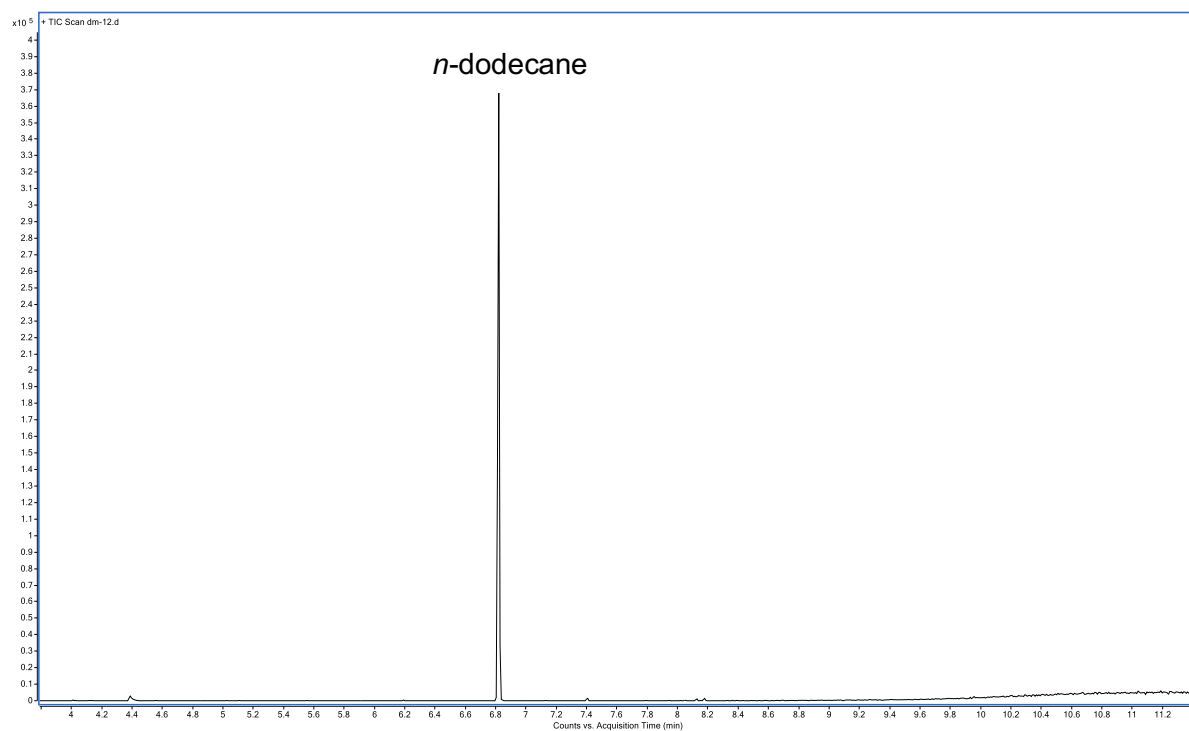


Figure S34. GCMS trace for 1-octene, Et₃SiH, **Sn1-Ir** (cat) in toluene at 80 °C, 24 h.

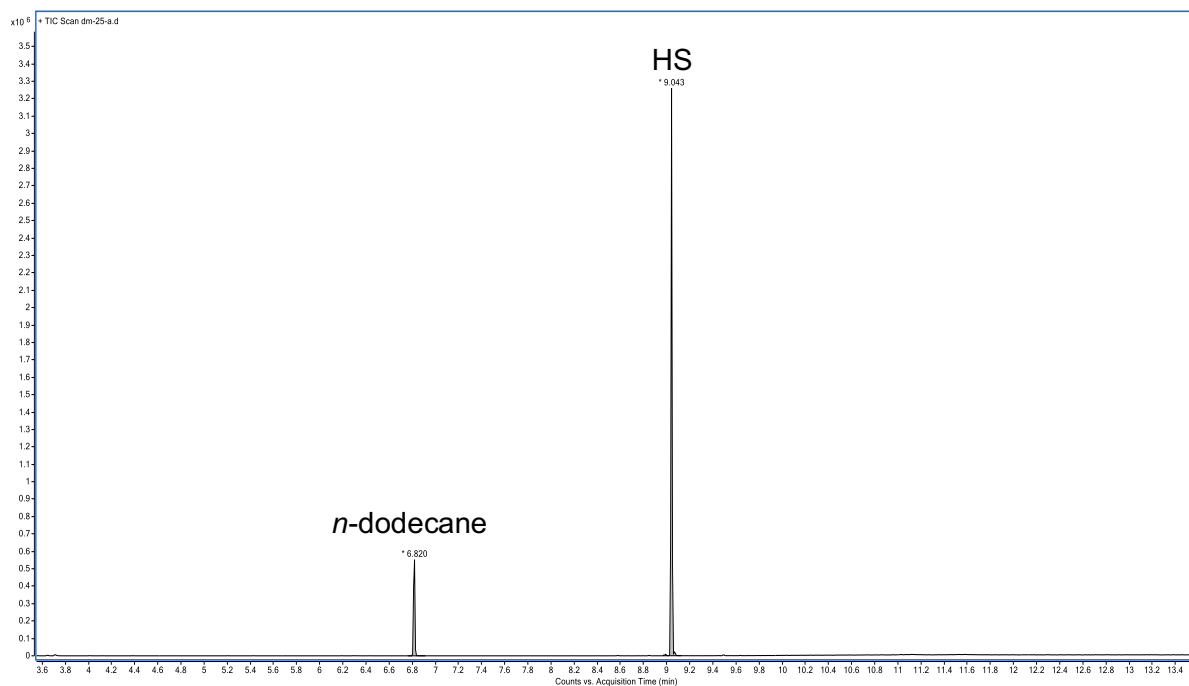


Figure S35. GCMS trace for 1-octene, PhMe₂SiH, **C1-Rh** (cat) in toluene at 80 °C, 24 h.

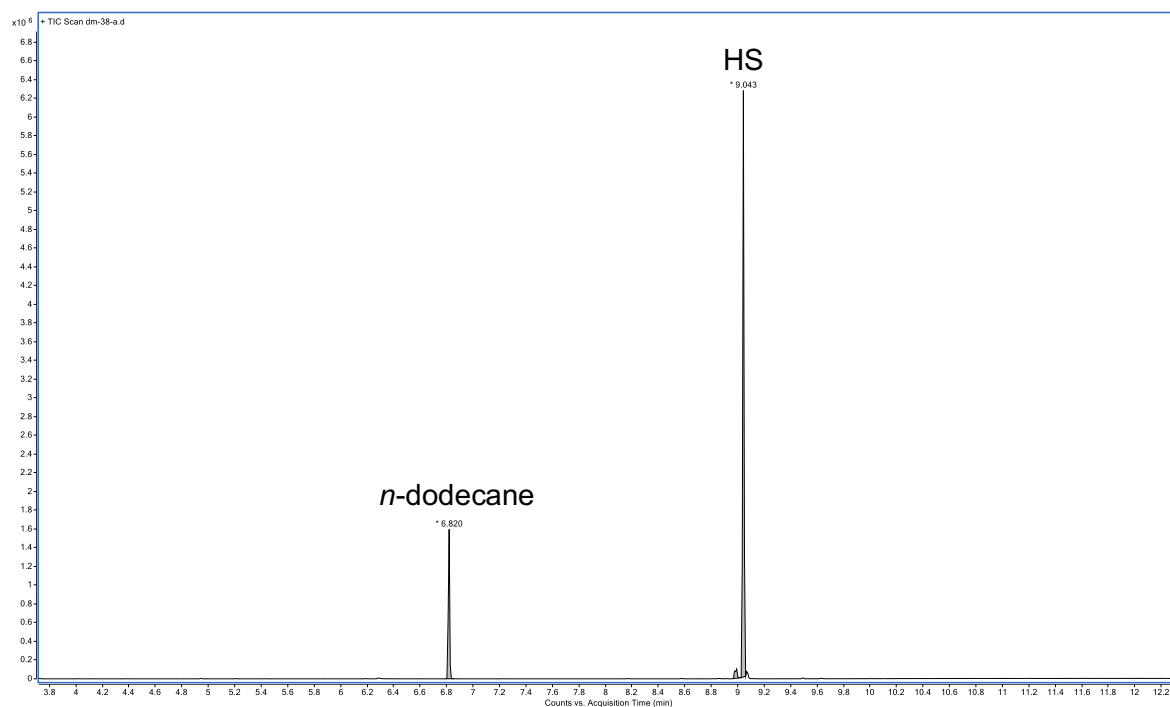


Figure S36. GCMS trace for 1-octene, PhMe₂SiH, Sn1-Rh (cat) in toluene at 80 °C, 24 h.

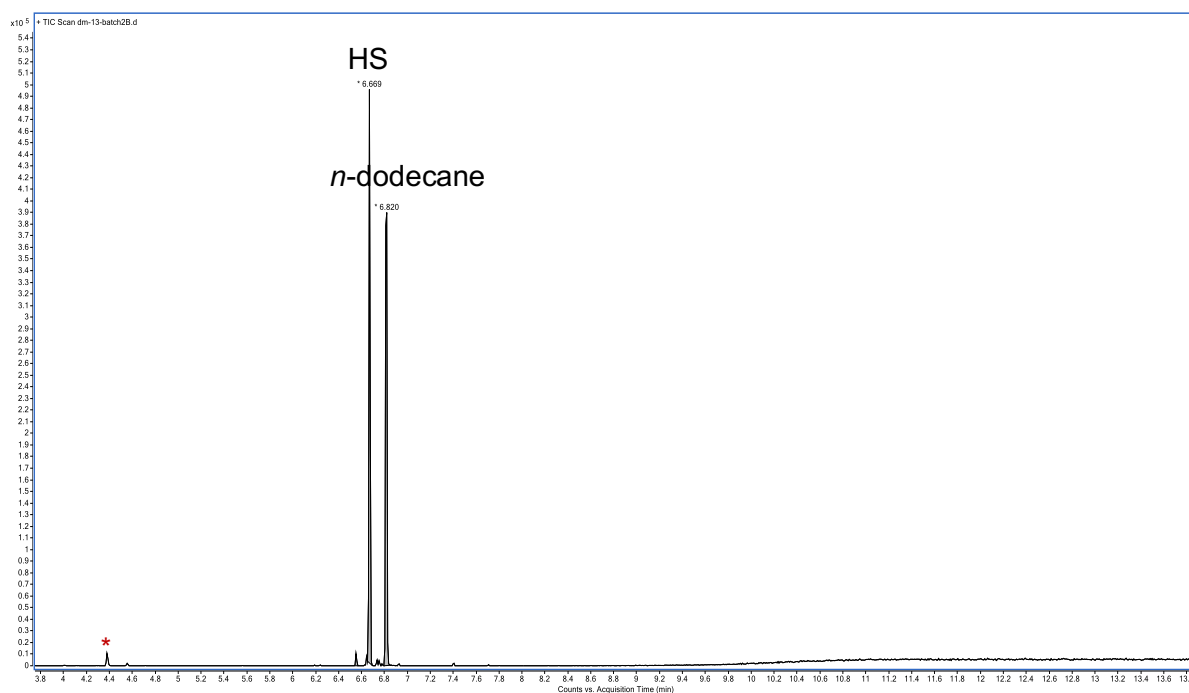


Figure S37. GCMS trace for 1-pentene, Et₃SiH, C1-Rh (cat) in toluene at 80 °C, 24 h (red asterisk = Hydrolysis product of Et₃SiH; HS = Hydrosilylation; DS = Dehydrogenative Silylation).

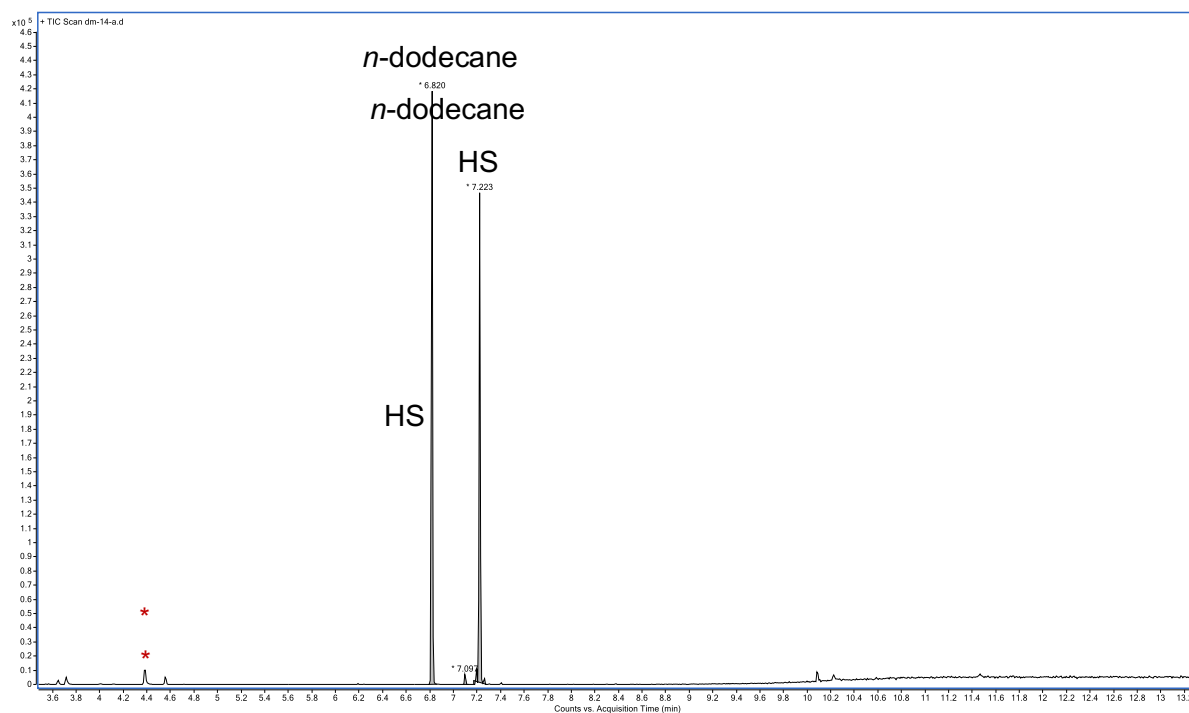


Figure S38. GCMS trace for 1-hexene, Et_3SiH , **C1-Rh** (cat) in toluene at 80°C , 24 h (red asterisk = Hydrolysis product of Et_3SiH ; HS = Hydrosilylation; DS = Dehydrogenative Silylation).

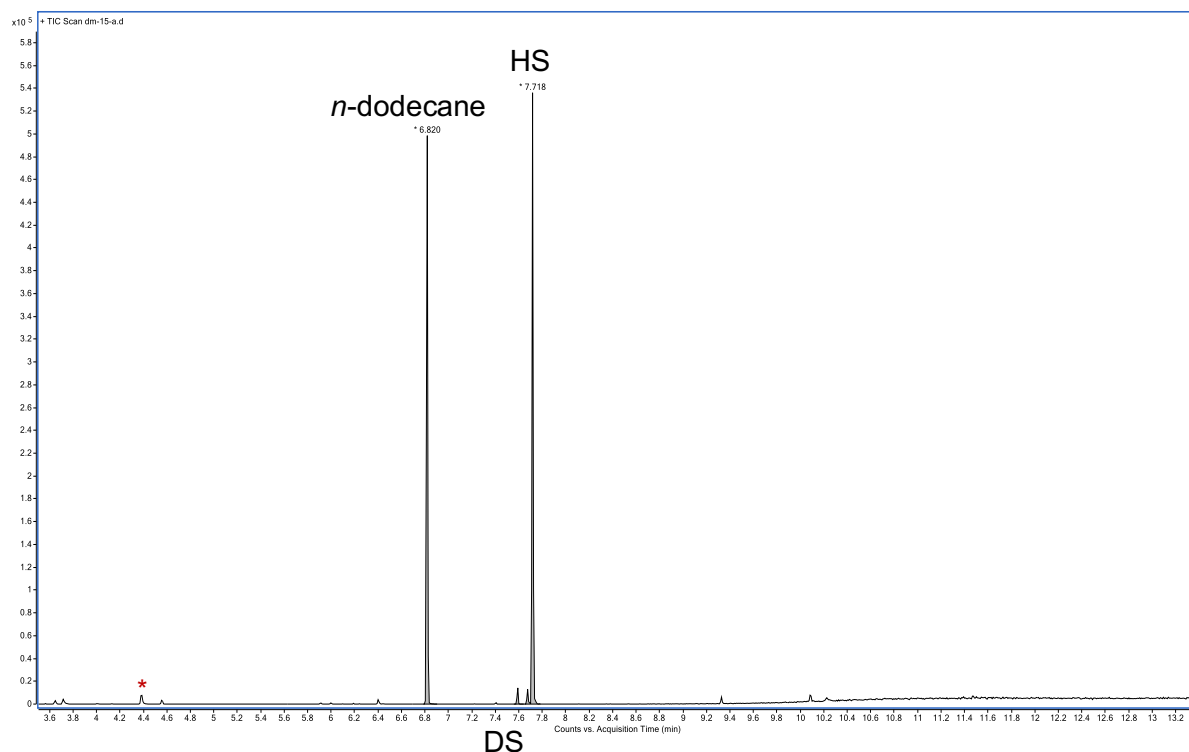


Figure S39. GCMS trace for 1-heptene, Et_3SiH , **C1-Rh** (cat) in toluene at 80°C , 24 h (red asterisk = Hydrolysis product of Et_3SiH ; HS = Hydrosilylation; DS = Dehydrogenative Silylation).

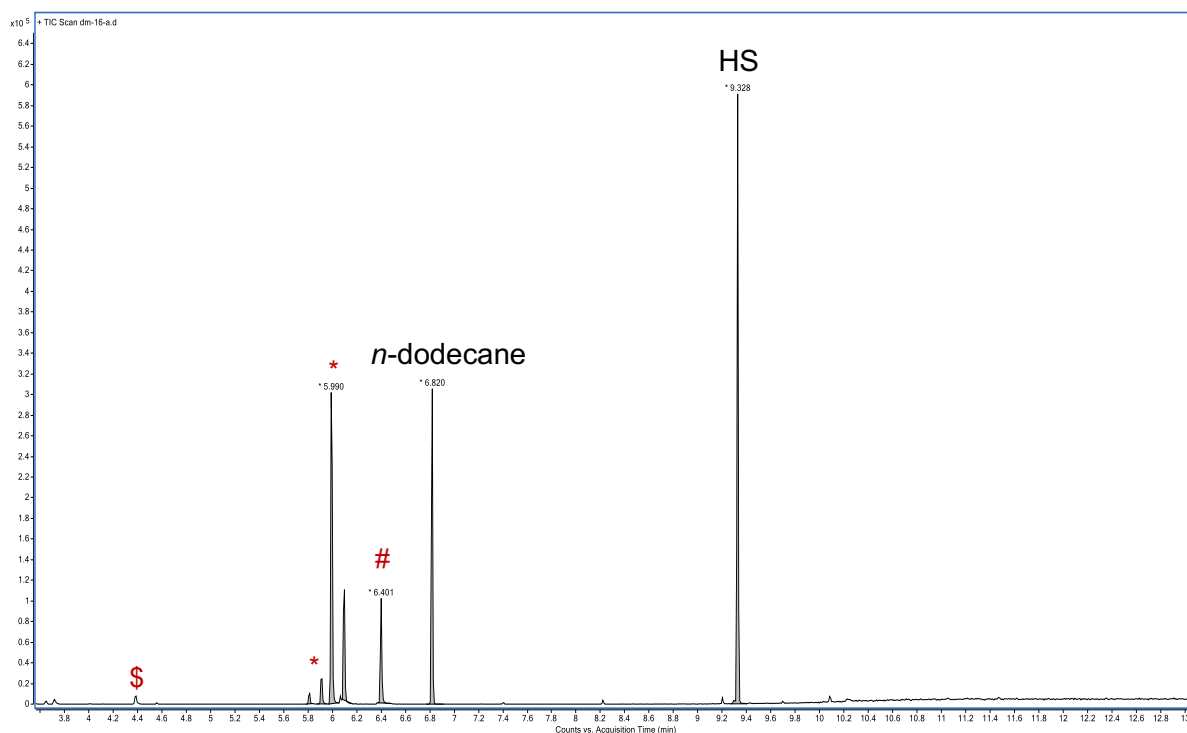


Figure S40. GCMS trace for 4-phenyl-1-butene, Et_3SiH , **C1-Rh** (cat) in toluene at 25 °C, 24 h (\$ = Hydrolysis product of Et_3SiH ; # = Unreacted alkene; * = Isomerised/hydrogenated alkenes).

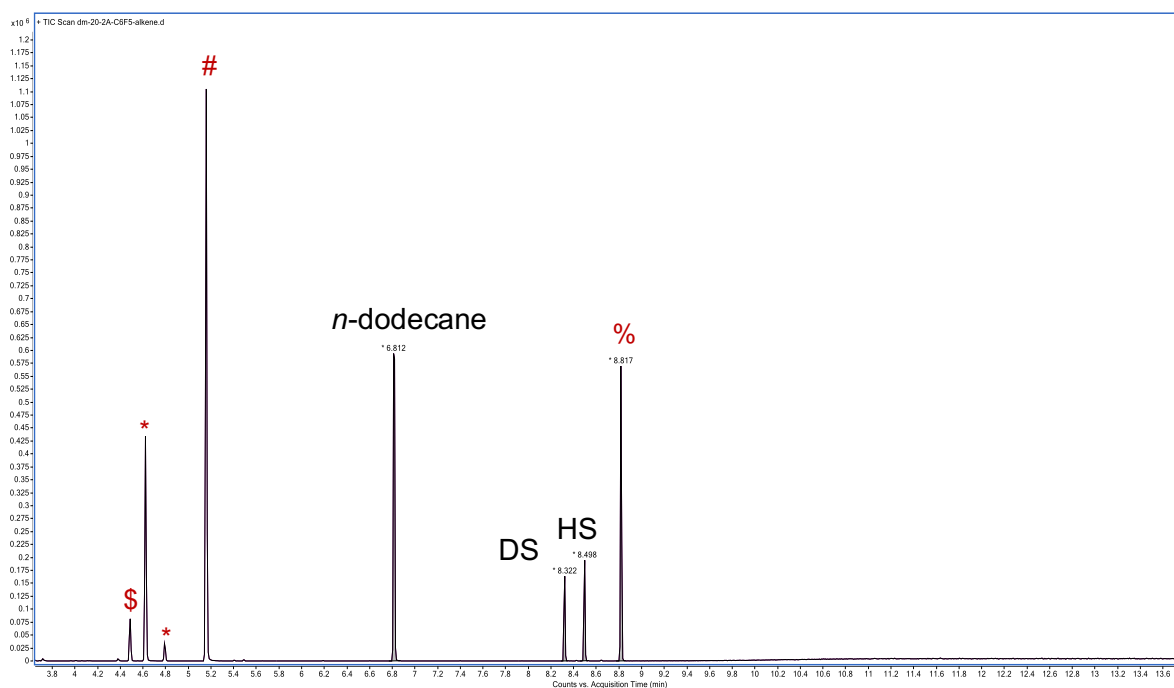


Figure S41. GCMS trace for allylpentafluorobenzene, Et_3SiH , **C1-Rh** (cat) in toluene at 25 °C, 24 h (\$ = Hydrolysis product of Et_3SiH ; # = Unreacted alkene; * = Isomerised/hydrogenated alkenes; % = Unidentified product).

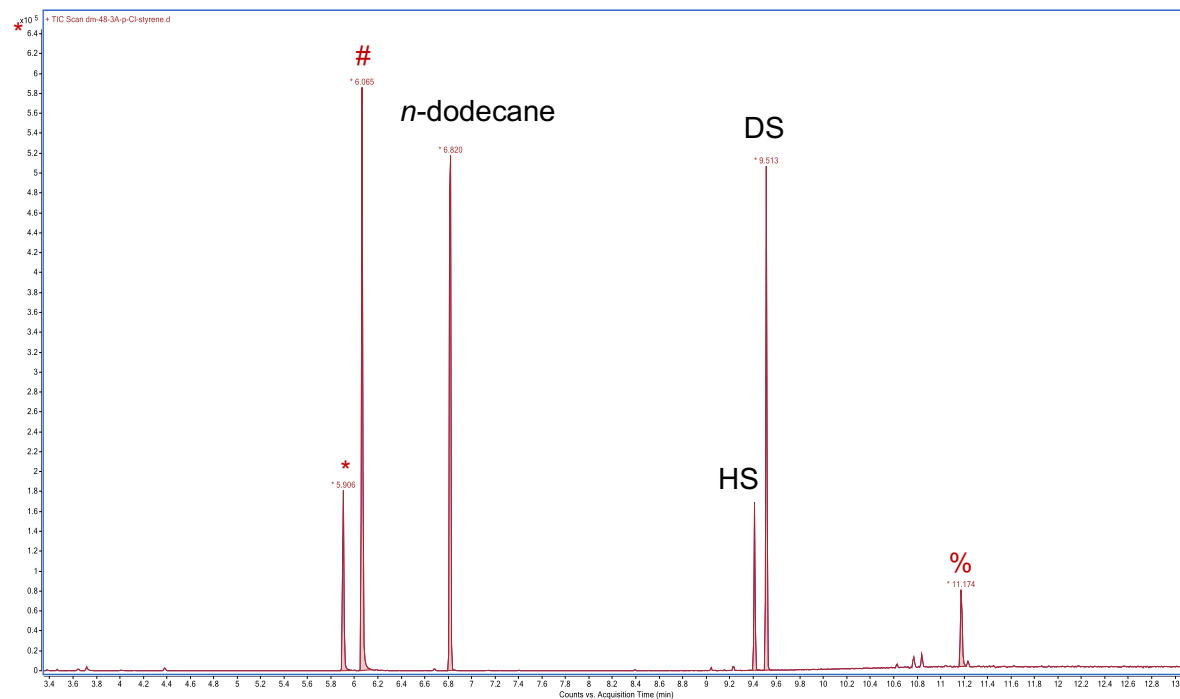


Figure S42. GCMS trace for 4-chloro-styrene, Et₃SiH, C1-Rh (cat) in toluene at 80 °C, 24 h (# = Unreacted alkene; * = Isomerised/hydrogenated alkenes; % = Unidentified product).

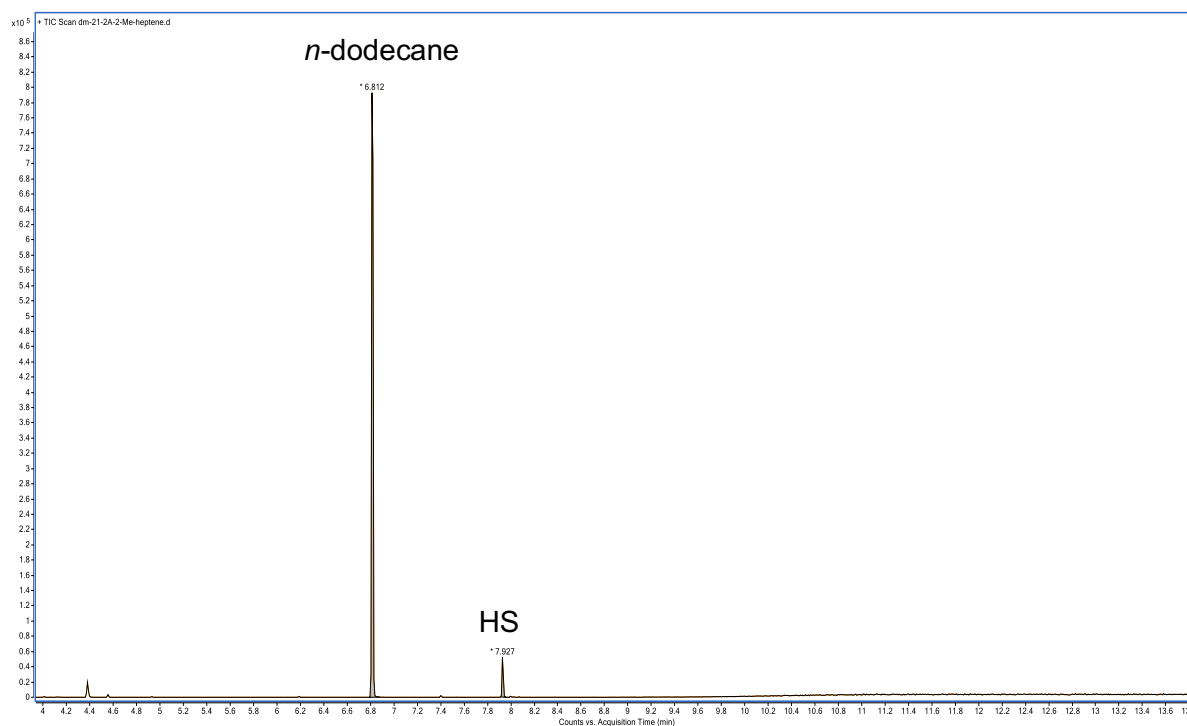


Figure S43. GCMS trace for α-methyl heptene, Et₃SiH, C1-Rh (cat) in toluene at 80 °C, 24 h.

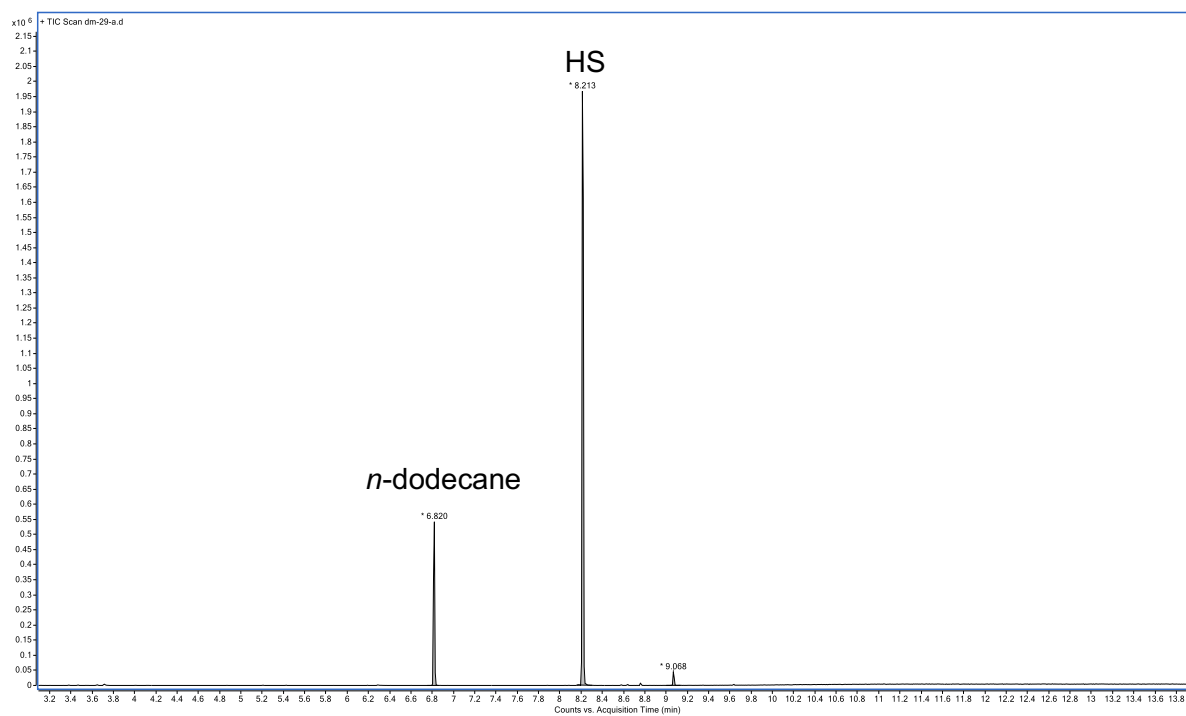


Figure S44. GCMS trace for 1-hexene, PhMe₂SiH, C1-Rh (cat) in toluene at 80 °C, 24 h.

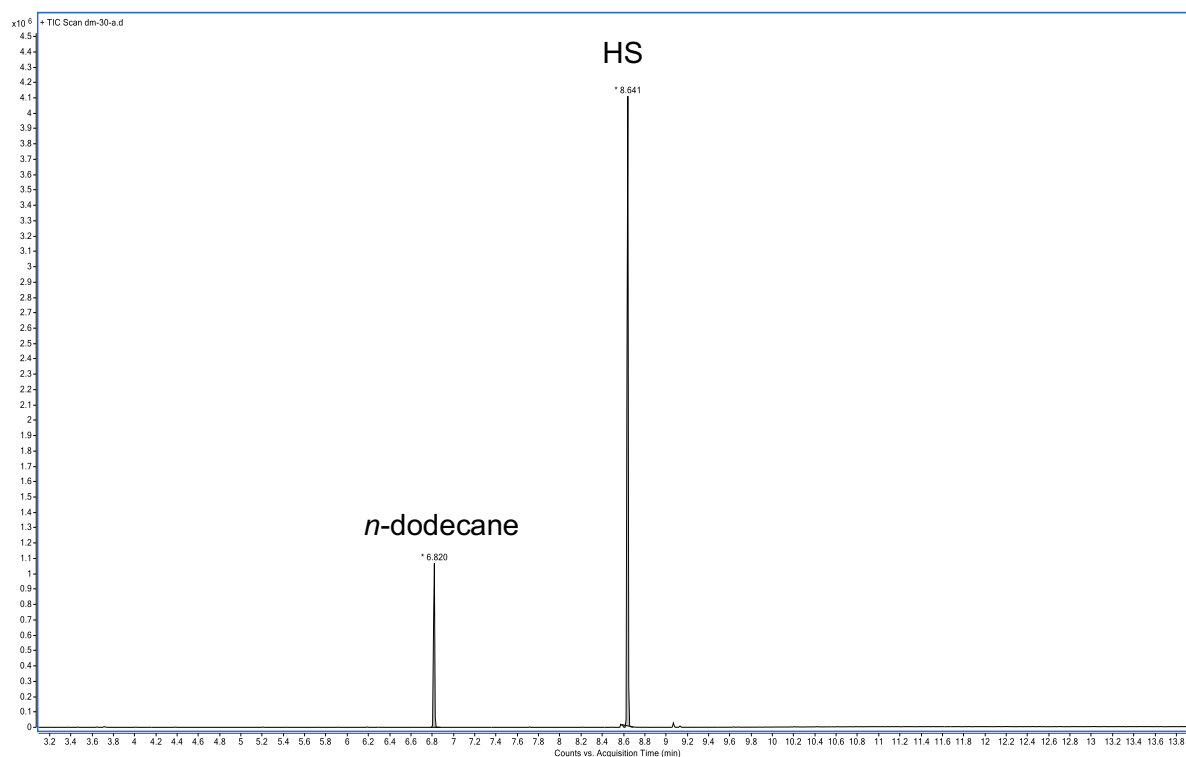


Figure S45. GCMS trace for 1-heptene, PhMe₂SiH, C1-Rh (cat) in toluene at 80 °C, 24 h.

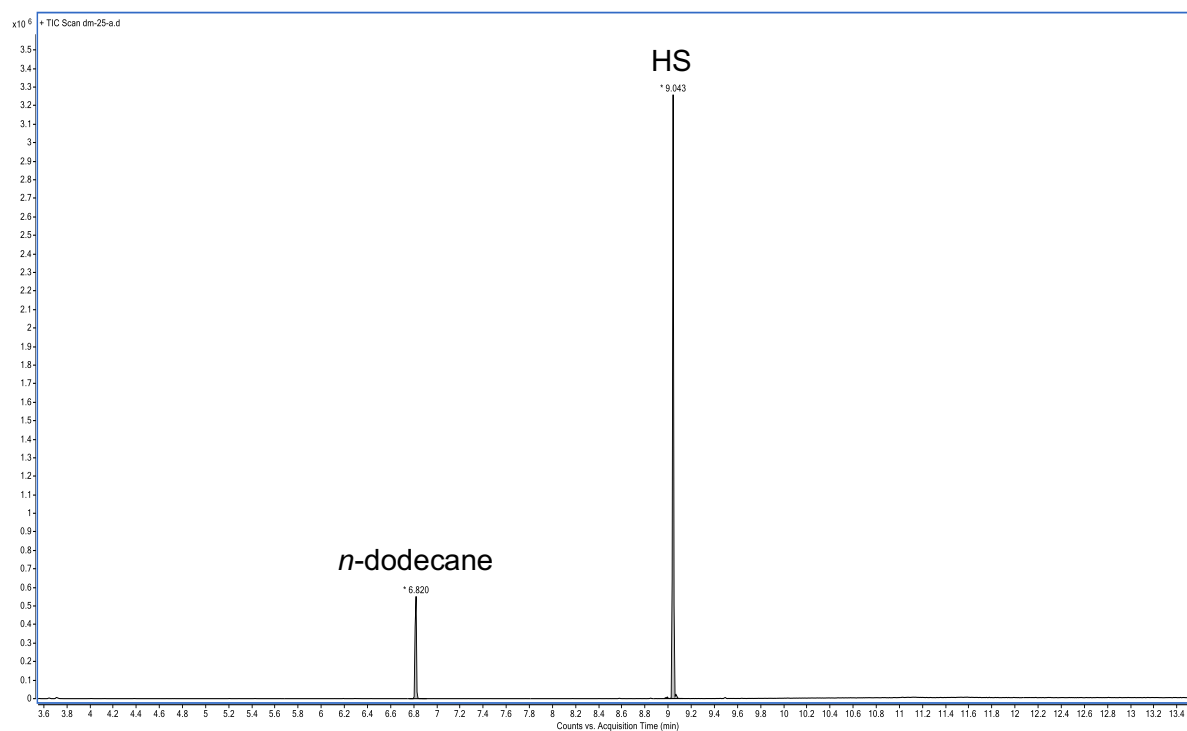


Figure S46. GCMS trace for 1-octene, PhMe₂SiH, **C1-Rh** (cat) in toluene at 80 °C, 24 h.

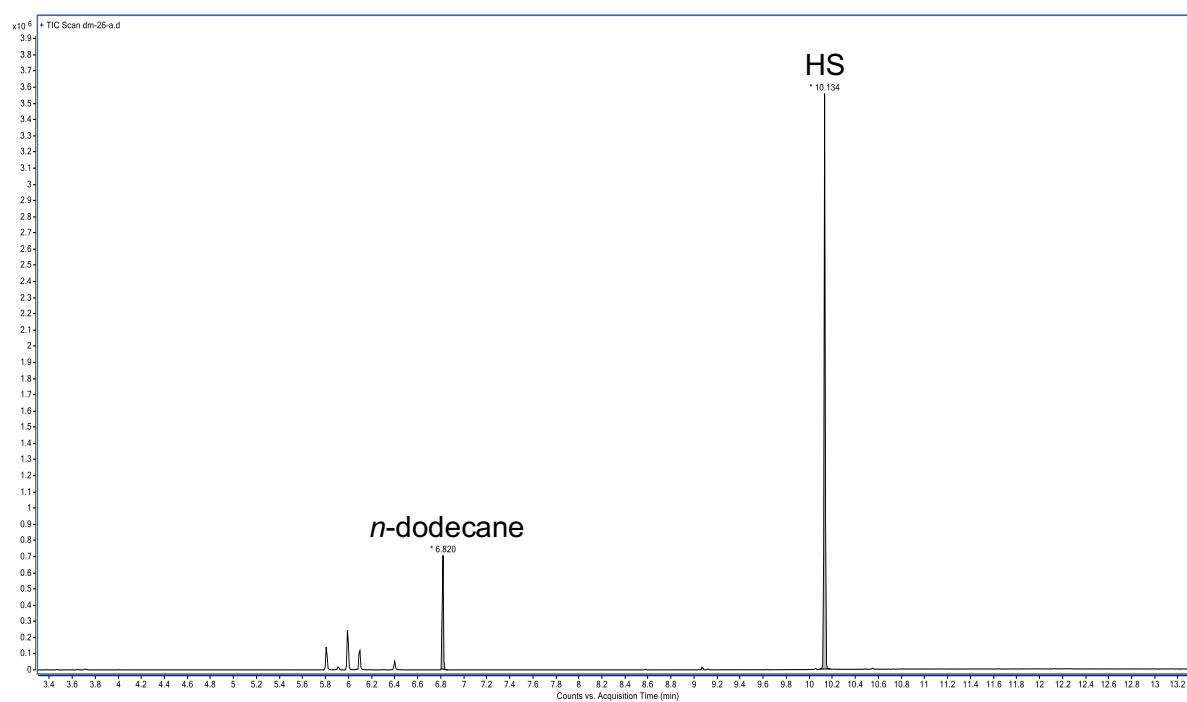


Figure S47. GCMS trace for 4-phenyl-1-butene, PhMe₂SiH, **C1-Rh** (cat) in toluene at 80 °C, 24 h.

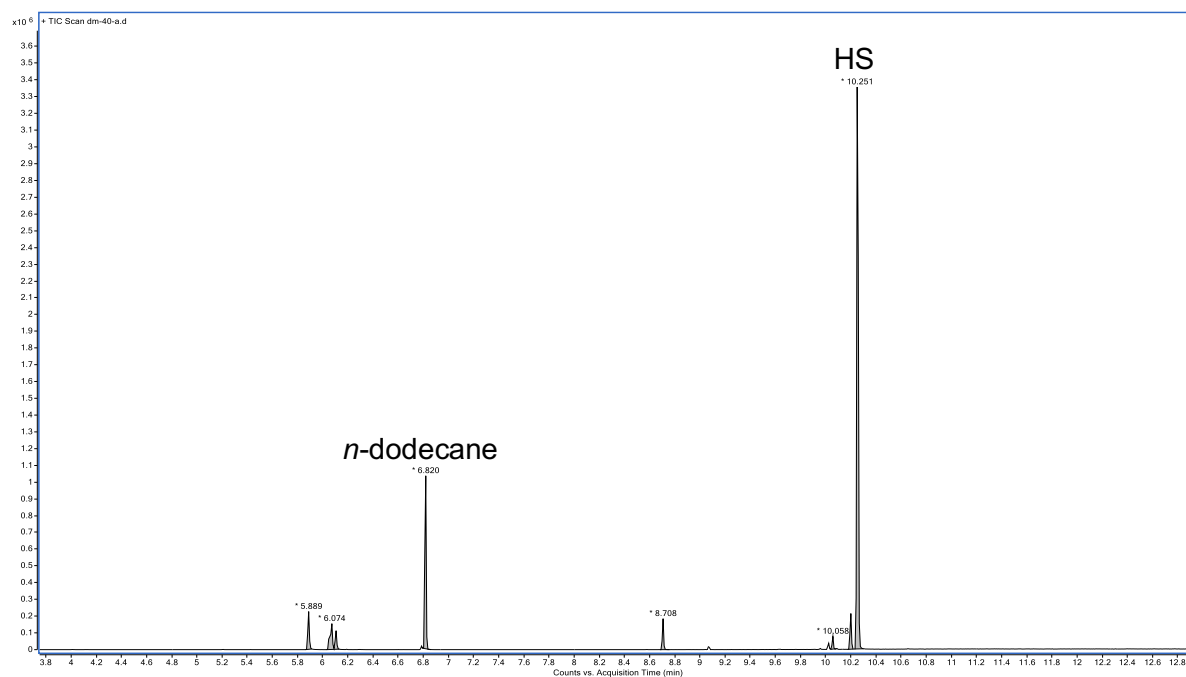


Figure S48. GCMS trace for 3-phenoxypropene, PhMe₂SiH, **C1-Rh** (cat) in toluene at 80 °C, 24 h.

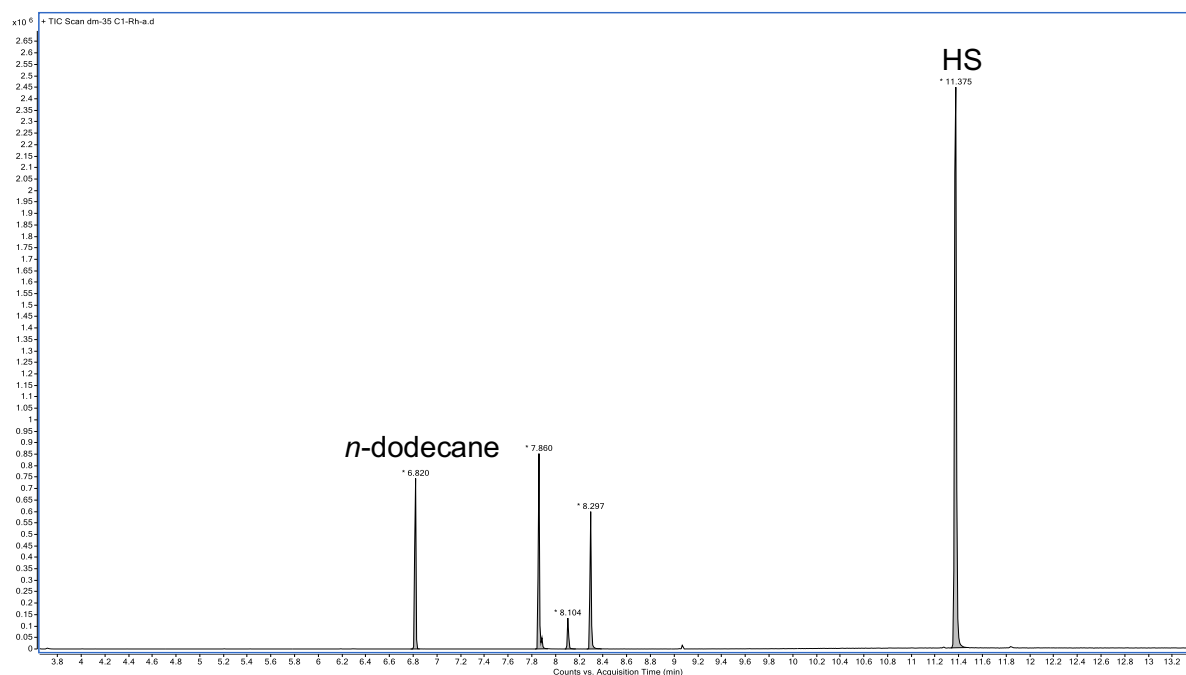


Figure S49. GCMS trace for methyl eugenol, PhMe₂SiH, **C1-Rh** (cat) in toluene at 80 °C, 24 h.

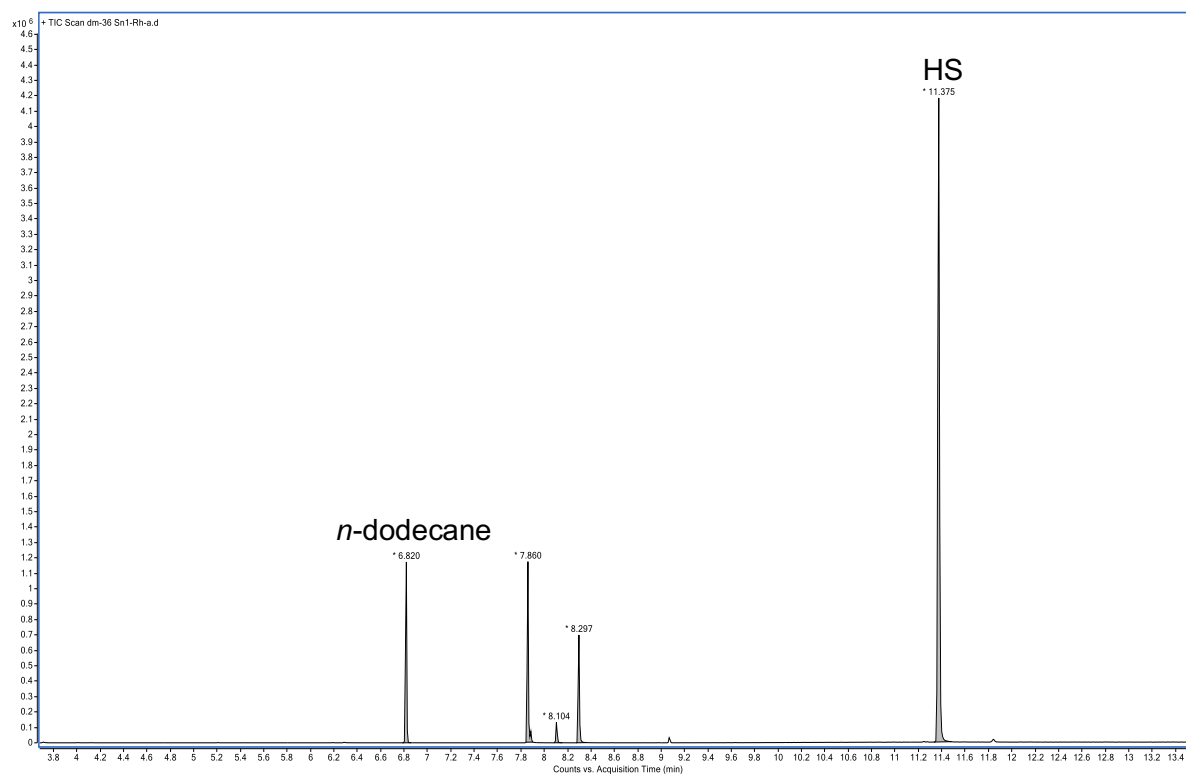


Figure S50. GCMS trace for methyl eugenol, $\text{Ph}(\text{Me})_2\text{SiH}$, **Sn1-Rh** (cat) in toluene at 80 °C, 24 h.

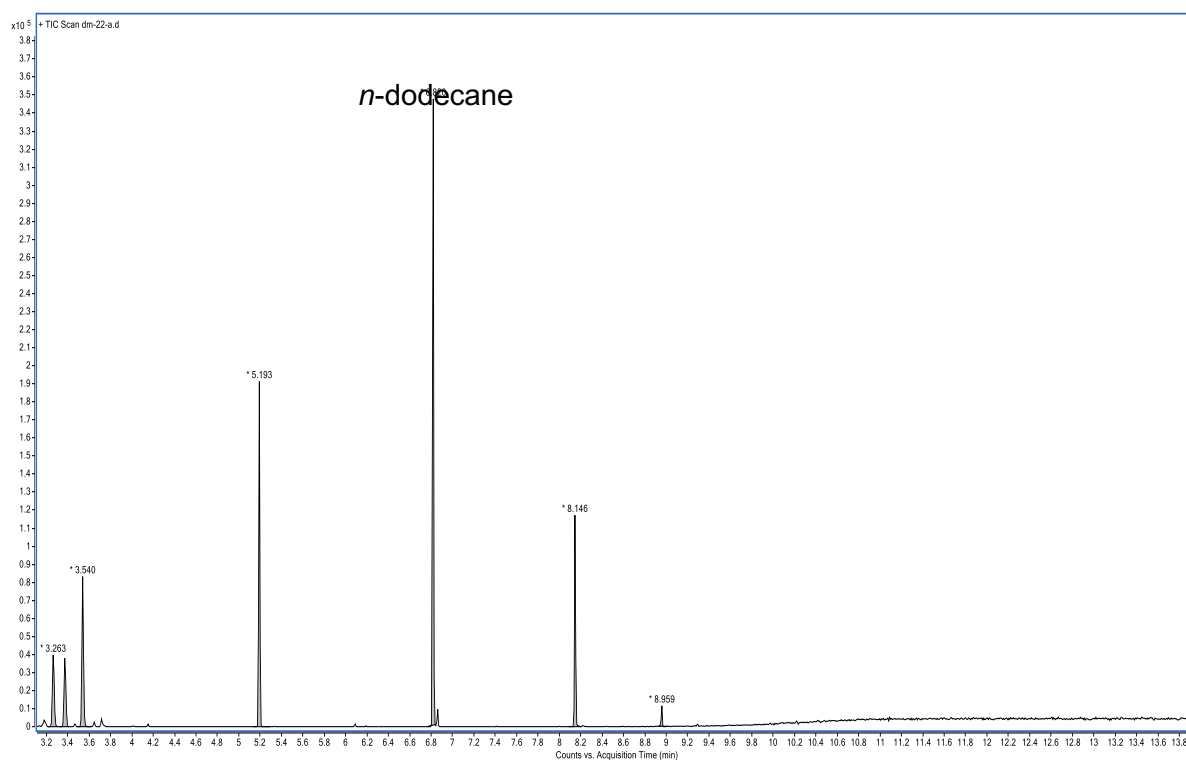


Figure S51. GCMS trace for 1-octene, $(\text{EtO})_3\text{SiH}$, **C1-Rh** (cat) in toluene at 80 °C, 24 h.

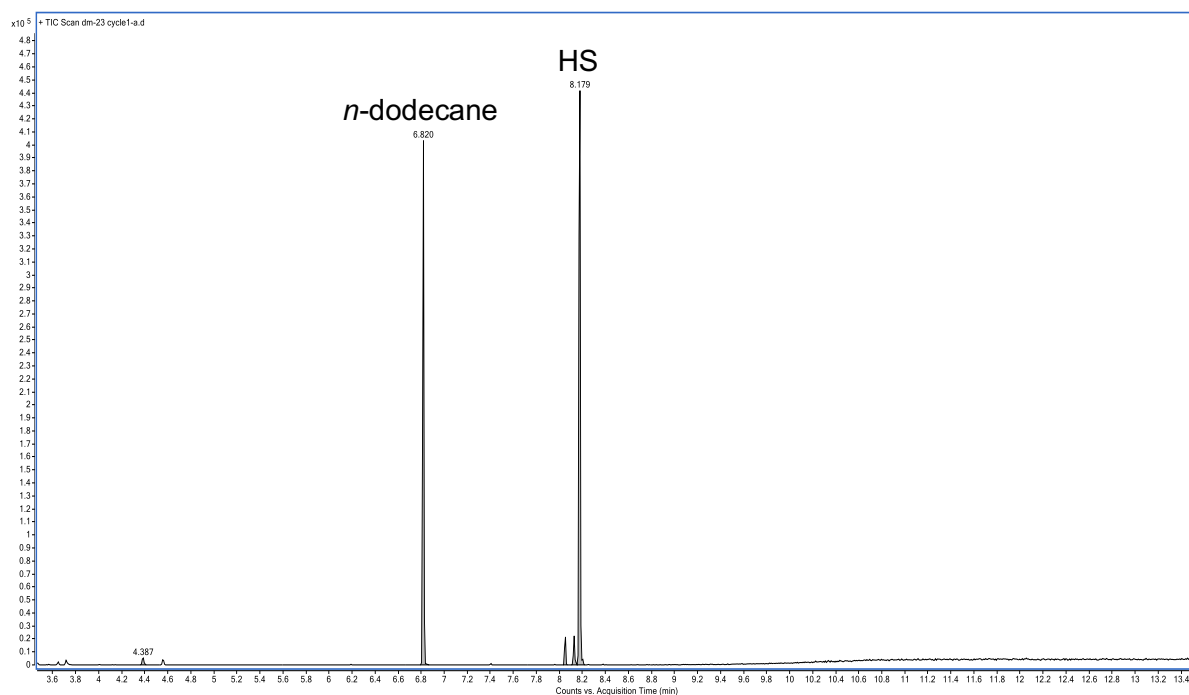


Figure S52. GCMS trace for **Cycle-I**: 1-octene, Et₃SiH, **C1-Rh** (cat) in toluene at 80 °C, 24 h.

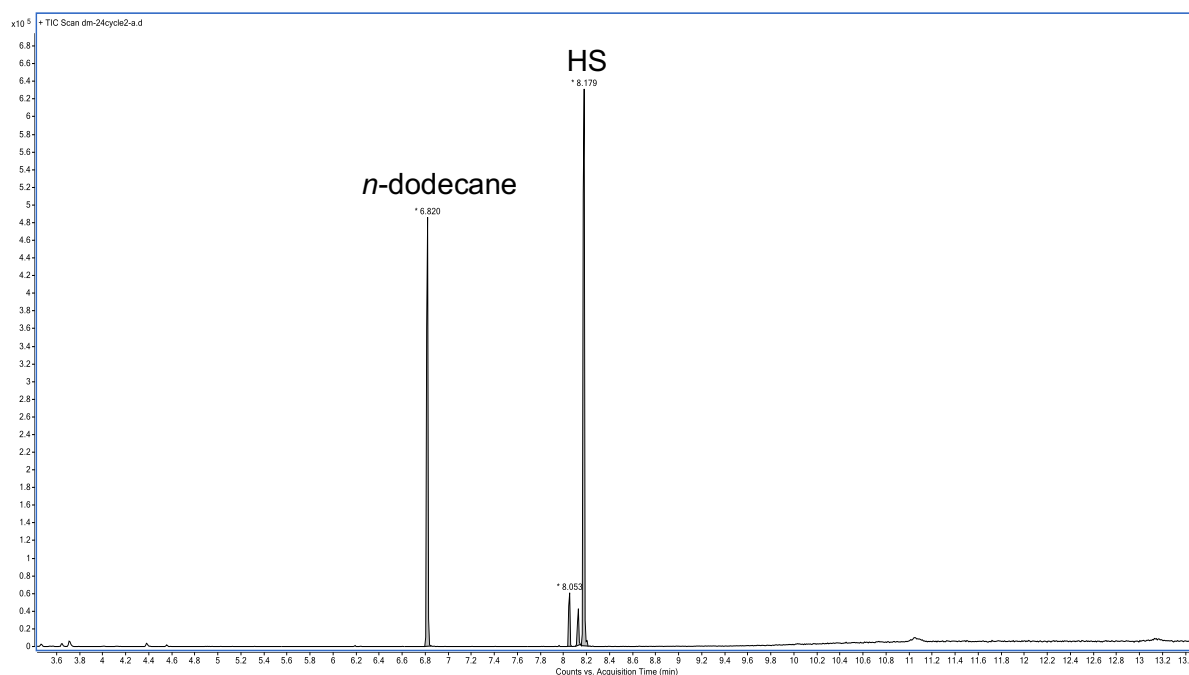


Figure S53. GCMS trace for **Cycle-II**: 1-octene, Et₃SiH, **C1-Rh** (cat) in toluene at 80 °C, 24 h.

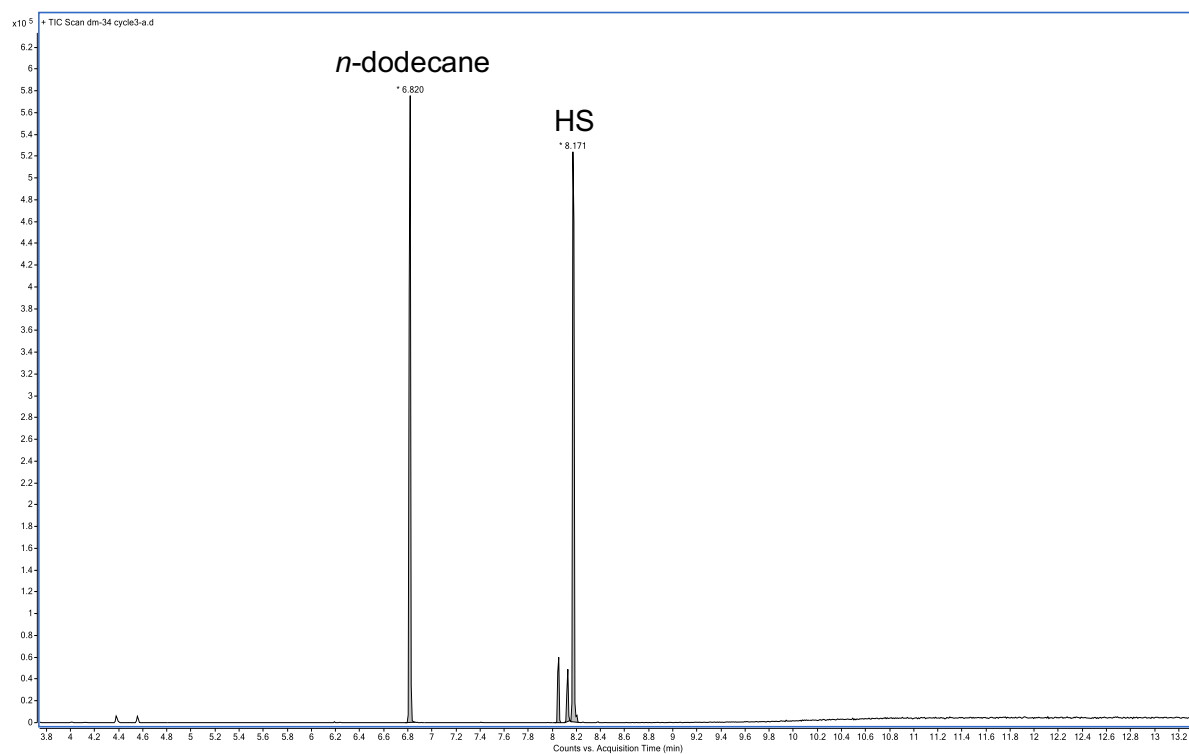


Figure S54. GCMS trace for **Cycle-III**: 1-octene, Et₃SiH, **C1-Rh** (cat) in toluene at 80 °C, 24 h.

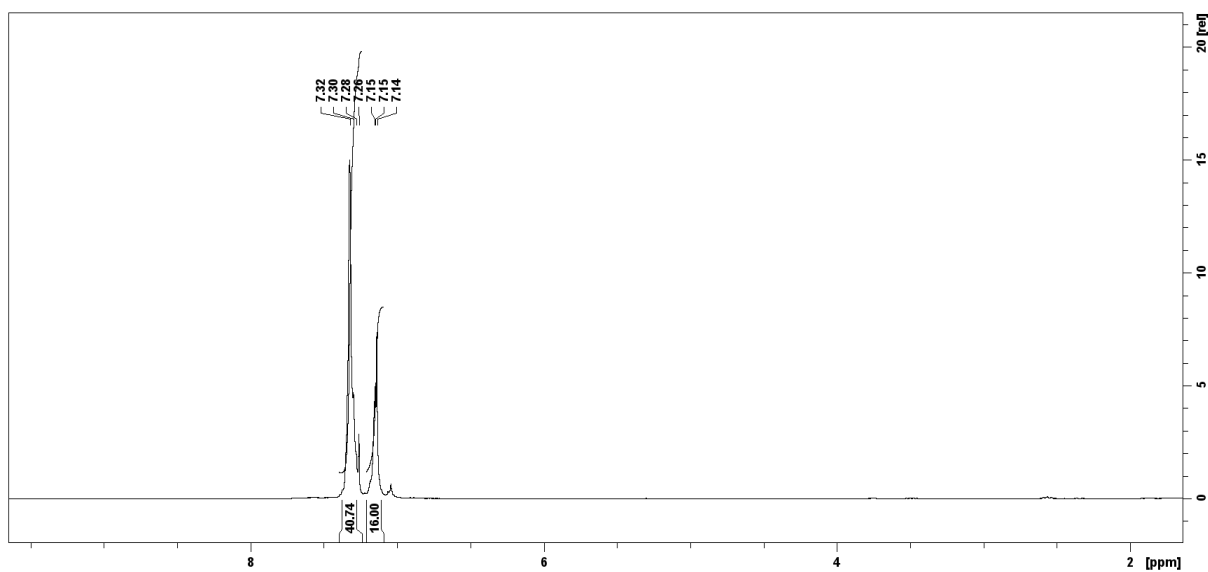


Figure S55. ¹H NMR (300 MHz) spectrum of the **C1** in CDCl₃.

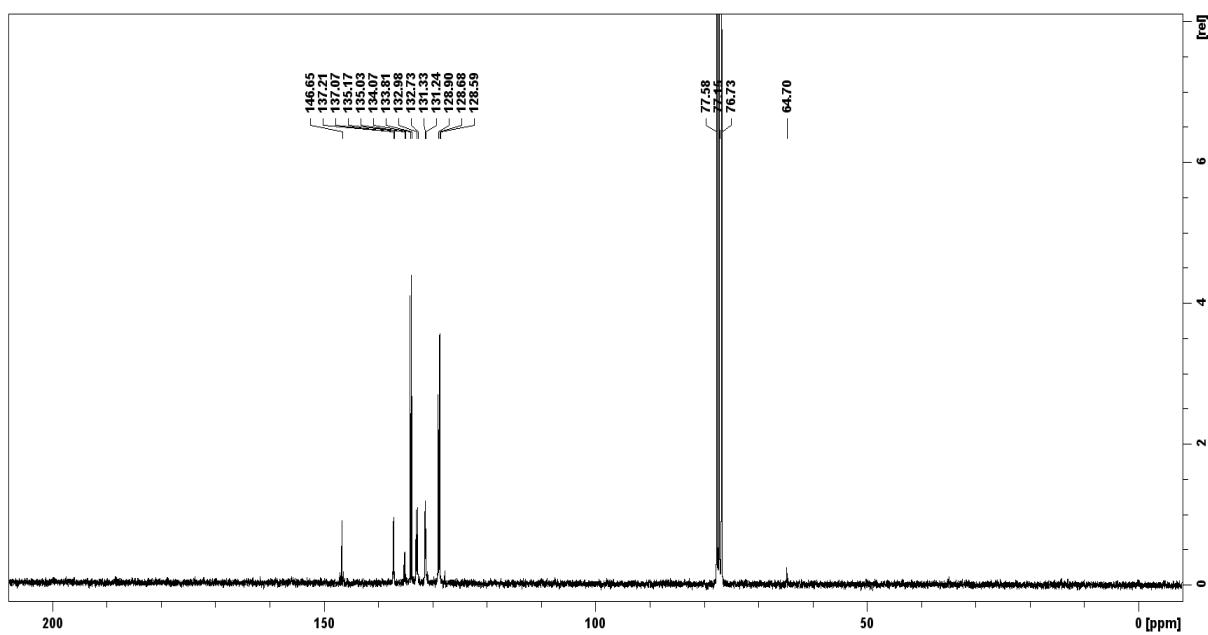


Figure S56. ¹³C{¹H} NMR (75 MHz) spectrum of the **C1** in CDCl₃.

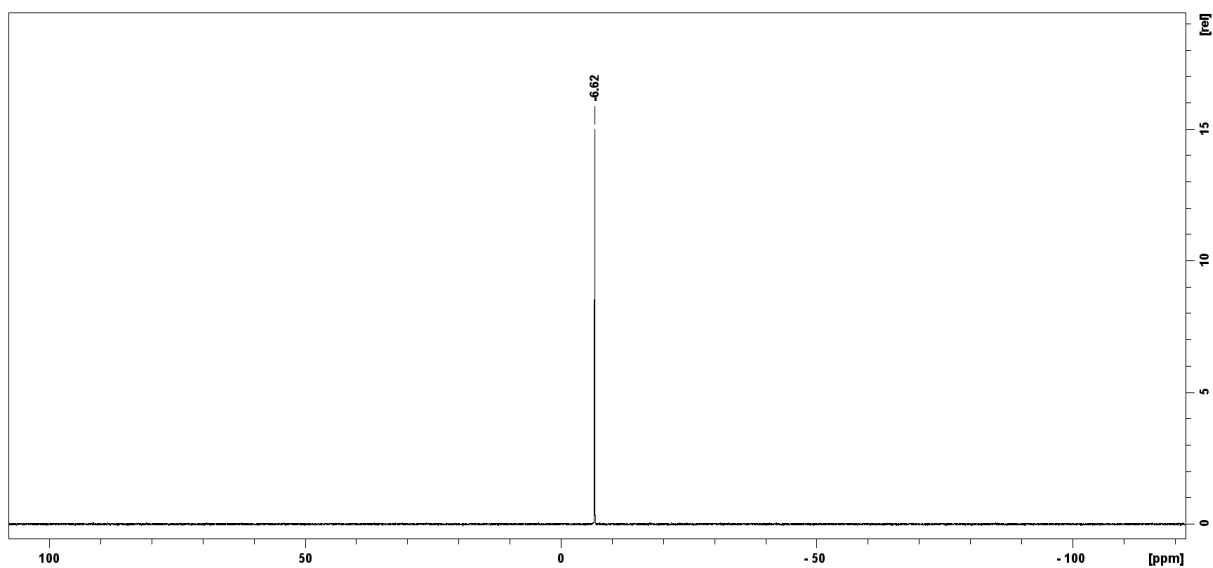


Figure S57. $^{31}\text{P}\{^1\text{H}\}$ NMR (122 MHz) spectrum of the **C1** in CDCl_3 .

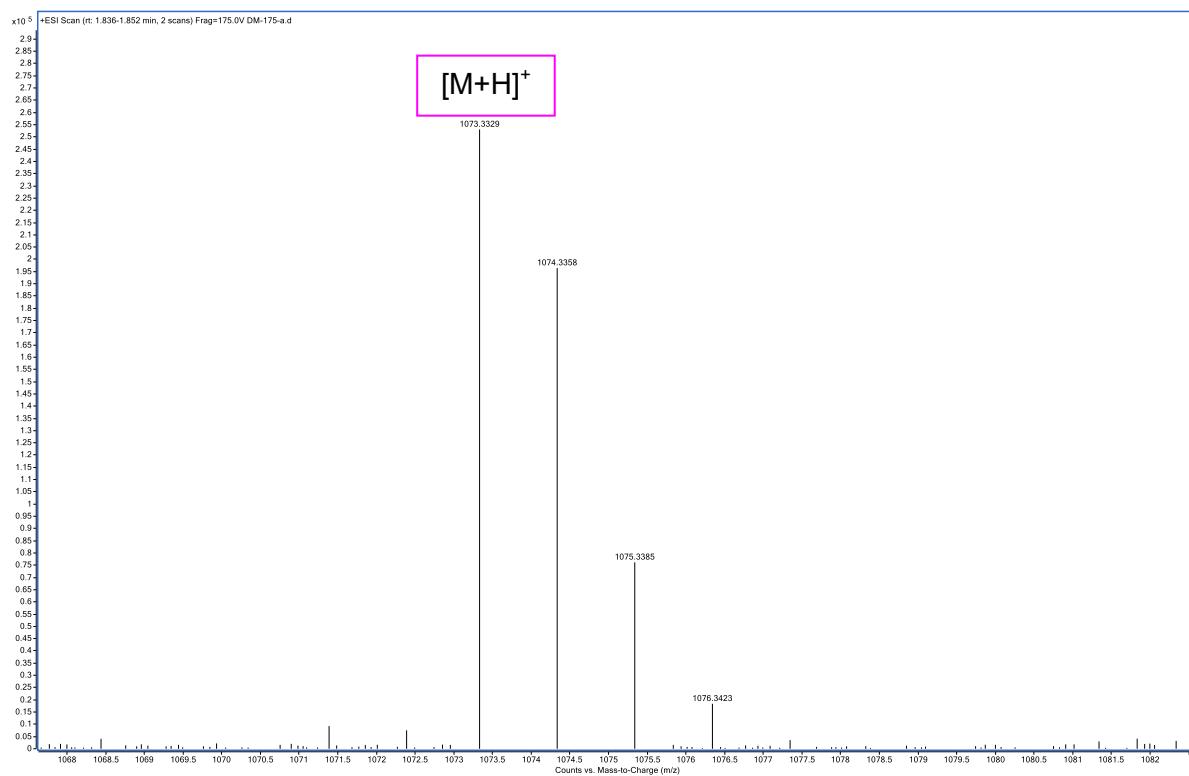


Figure S58. HR-ESI-TOFMS (positive mode) of **C1**.

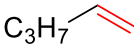
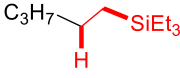
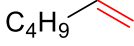
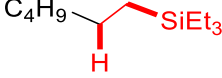
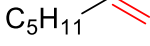
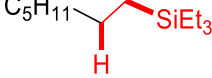
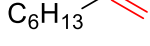
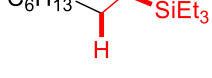
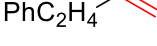
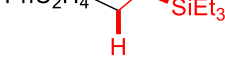
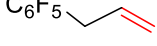
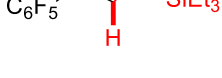
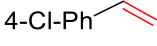
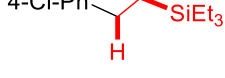
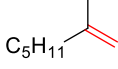
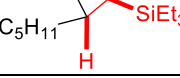
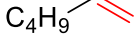
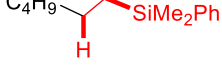
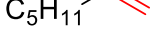
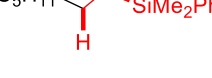
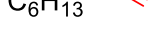
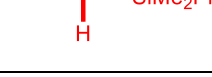
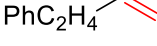
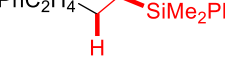
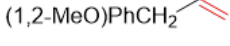
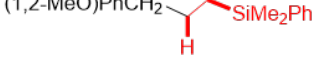
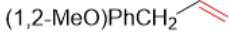
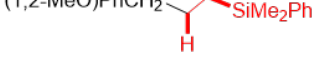
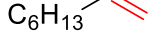
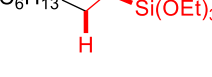
Supplementary Tables

Table S1. Detail optimization for the catalytic conversion of 1-octene.

Entry	Catalyst	Solvent	Temp, Time	Yield HS (%) ^a	Yield DS (%) ^a
1	-	Toluene	80 °C, 24h	0%	0%
2	C1-Rh	Toluene	25 °C, 24h	<1%	<1%
3 ^b	C1-Rh	Toluene	80 °C, 24h	39±1	3±1%
4	C1-Rh	Benzene	80 °C, 24h	40%	3%
5	C1-Rh	THF	70 °C, 24h	22%	2%
6	C1-Rh	CDCl ₃	70 °C, 24h	23%	3%
7	C1-Ir	Toluene	80 °C, 24h	0%	0%
8 ^b	[Rh(CO)Cl(PPh₃)₂]	Toluene	80 °C, 24h	4±2%	3±1%
9 ^b	[RhCl(PPh₃)₃]	Toluene	80 °C, 24h	28±3%	2±2%
10	Sn1-Rh	Toluene	80 °C, 24h	30%	5%
11	Sn1-Ir	Toluene	80 °C, 24h	0%	0%
12 ^{c,d}	C1-Rh	Toluene	80 °C, 24h	>99	0%
13 ^c	Sn1-Rh	Toluene	80 °C, 24h	>99	0%

^a Yields were assessed by GCMS analysis using internal *n*-dodecane standard. ^b Yields are based on three independent experiments (*n* = 3). ^c Use of PhMe₂SiH instead of Et₃SiH. ^d Yields are based on two independent experiments (*n* = 2).

Table S2. Substrate cope of the hydrosilylation reaction using **C1-Rh** MOF as a catalyst.

Entry	Substrate	HS Product	Yield HS(%)	Yield DS(%)
1			31±8% (n = 3)	0% (n = 3)
2			28±5% (n = 3)	0% (n = 3)
3			37±3% (n = 3)	2±1% (n = 3)
4			39±1% (n = 3)	3±1% (n = 3)
5			85±9% (n = 3)	0% (n = 3)
6			11±2% (n = 2)	9±1% (n = 2)
7			9±1% (n = 2)	29±2% (n = 2)
8			2±1 (n = 3)%	0% (n = 3)
9			>99% (n=1)	0% (n=1)
10			>99% (n = 1)	0% (n = 1)
11			>99±0% (n = 2)	0% (n = 2)
12			>99% (n = 1)	0% (n = 1)
13			>99% (n = 1)	0% (n = 1)
14 ^a			>99% (n = 1)	0% (n = 1)
15			0% (n = 1)	0% (n = 1)

^a used **Sn1-Rh** as a catalyst.

Table S3. Crystal data, data collection and refinement parameters for the structure of **C1-Rh**.

Identification code	C1-Rh
CCDC Number	2419327
Empirical formula	$C_{300}H_{224}Cl_8O_8P_{16}Rh_8$
Formula weight	5559.18
Temperature/K	100.15
Crystal system	orthorhombic
Space group	<i>Fddd</i>
<i>a</i> /Å	11.6257(6)
<i>b</i> /Å	22.2356(13)
<i>c</i> /Å	46.905(3)
α /°	90
β /°	90
γ /°	90
Volume/Å ³	12125.0(12)
<i>Z</i>	2
ρ_{calc} /cm ³	1.523
μ /mm ⁻¹	0.788
<i>F</i> (000)	5648.0
Crystal size/mm ³	0.033 × 0.014 × 0.01
Radiation	MoK α (λ = 0.71073)
2 θ range for data collection/°	3.474 to 50.69
Index ranges	-12 ≤ <i>h</i> ≤ 14, -26 ≤ <i>k</i> ≤ 23, -56 ≤ <i>l</i> ≤ 55
Reflections collected	13932
Independent reflections	2773 R_{int} = 0.0497, R_{sigma} = 0.0428]
Data/restraints/parameters	2773/362/298
Goodness-of-fit on F^2	1.134
Final <i>R</i> indexes [$I \geq 2\sigma(I)$]	R_1 = 0.0722, wR_2 = 0.1944
Final <i>R</i> indexes [all data]	R_1 = 0.0965, wR_2 = 0.2129
Largest diff. peak/hole / e Å ⁻³	1.85/-0.44

Table S4. Crystal data, data collection and refinement parameters for the structure of **C1-Ir**.

Identification code	C1-Ir
CCDC Number	2419328
Empirical formula	C ₃₀₀ H ₂₂₄ Cl ₈ Ir ₈ O ₈ P ₁₆
Formula weight	6273.50
Temperature/K	100.00
Crystal system	orthorhombic
Space group	<i>Fddd</i>
<i>a</i> /Å	11.573(2)
<i>b</i> /Å	22.229(4)
<i>c</i> /Å	46.579(10)
<i>α</i> /°	90
<i>β</i> /°	90
<i>γ</i> /°	90
Volume/Å ³	11983(4)
<i>Z</i>	2
ρ_{calc} /cm ³	1.739
μ /mm ⁻¹	4.684
<i>F</i> (000)	6160.0
Crystal size/mm ³	0.08 × 0.06 × 0.03
Radiation	MoK α (λ = 0.71073)
2 θ range for data collection/°	4.06 to 49.586
Index ranges	-13 ≤ <i>h</i> ≤ 10, -26 ≤ <i>k</i> ≤ 25, -54 ≤ <i>l</i> ≤ 54
Reflections collected	22455
Independent reflections	2588 [<i>R</i> _{int} = 0.0728, <i>R</i> _{sigma} = 0.0479]
Data/restraints/parameters	2588/356/298
Goodness-of-fit on <i>F</i> ²	1.124
Final <i>R</i> indexes [<i>I</i> ≥ 2 σ (<i>I</i>)]	<i>R</i> ₁ = 0.0645, <i>wR</i> ₂ = 0.1589
Final <i>R</i> indexes [all data]	<i>R</i> ₁ = 0.0947, <i>wR</i> ₂ = 0.1761
Largest diff. peak/hole / e Å ⁻³	2.38/-1.12